Switching of N-Methyl-D-aspartate (NMDA) Receptor-favorite Intracellular Signal Pathways from ERK1/2 Protein to p38 Mitogen-activated Protein Kinase Leads to Developmental Changes in NMDA Neurotoxicity*

Lin Xiao(肖 林)[‡1], **Chun Hu**(胡 春)[‡], **Chunzhi Feng**(冯 春 芝)[§], **and Yizhang Chen**(陈 宜 张)[‡2]

From the ‡Institute of Neuroscience, Key Laboratory of Molecular Neurobiology, Ministry of Education; Neuroscience Center of Changzheng Hospital, Second Military Medical University, Shanghai 200433 and §University Hospital, Fudan University, Shanghai 200433, China

Excitotoxicity mediated by overactivation of N-methyl-D-aspartate receptors (NMDARs) has been implicated in a variety of neuropathological conditions in the central nervous system (CNS). It has been suggested that N-methyl-D-aspartate (NMDA) neurotoxicity is developmentally regulated, but the definite pattern of the regulation has been controversial, and the underlying mechanism remains largely unknown. Here, we show that NMDA treatment leads to significant cell death in mature (9 and 12 days in vitro) hippocampal neurons or hippocampi of young postnatal day 12 and adult rats but not in immature (3 and 6 days in vitro) neurons or embryonic day 18 and neonatal rat hippocampi. In contrast, NMDA promotes survival of immature neurons against tropic deprivation. Interestingly, it is found that NMDA preferentially activates p38 MAPK in mature neuron and adult rat hippocampus, but it favors ERK1/2 activation in immature neuron and postnatal day 0 rat hippocampus. Moreover, it is shown that NMDA neurotoxicity in mature neuron is mediated via p38 MAPK activation, and neuroprotection in immature neuron is mediated via ERK1/2 activation, whereas all these effects are NR2B-containing NMDAR-dependent, as well as Ca^{2+}-dependent. We also revealed that mature and immature neurons showed no difference in the amplitude of NMDA-induced intracellular calcium ($[Ca^{2+}]_i$) increase. However, the basal level of $[Ca^{2+}]_i$ is shown to elevate with the maturation of neuron, and this elevation is attributable to the changes in NMDA neurotoxicity but not to the switch of the NMDAR signaling pathway. Taken together, our results suggest that a switch of NMDA receptor-favorite intracellular signal pathways from ERK1/2 to p38 MAPK and the elevated basal level of $[Ca^{2+}]_i$ with age might be critical for the developmental changes in NMDA neurotoxicity in the hippocampal neuron.

Glutamate is the major excitatory neurotransmitter in the mammalian central nervous system (CNS). Glutamatergic transmission is mediated by two types of receptors classified primarily in terms of their pharmacological characteristics, namely ionotropic glutamate receptors and metabotropic glutamate receptors. Ionotropic glutamate receptors consist of three subtypes as follows: N-methyl-D-aspartate receptor (NMDAR),[3] α-amino-3-hydroxy-5-methyl-4-isoxazolepropionic acid receptor and kainite receptor. Among them, NMDARs play crucial roles in a wide variety of physiological processes such as neuronal development, survival, and synaptic plasticity. But overactivation of NMDARs can lead to intensive excitotoxic neuronal death. It is the main mediator of brain injury following many acute neurological toxic insults, such as stroke, epileptic seizures, cerebral ischemia, and brain trauma (1, 2). It has also been implicated in the pathogenesis of a variety of chronic neurodegenerative disorders (1, 3), including Alzheimer (4), Parkinson (5), and Huntington disease (6). However, over-inhibition of NMDAR activity might also result in neuronal death especially in the developing brain, which may call attention to the cautious use of NMDAR blockers such as ketamine in pregnancy or pediatric anesthesia (7–9). Thus, NMDAR seems to exert a complex role by mediating both neurotoxic and neuroprotective effects in the CNS, although the detailed mechanism is still in debate (10, 11).

Functional NMDA receptors are heteromeric assemblies of the following four subunits: generally two NMDA-R1 and two NMDA-R2 subunits. Together, the four subunits form a channel in the plasma membrane permitting influx of Ca^{2+} when stimulated. The NMDA-R1 subunits (NR1) are derived from a single gene that can exist as eight different variants based on alternative splicing, whereas four separate genes encode the NMDA-R2 subunits (NR2A, NR2B, NR2C, and NR2D) that differ in channel conductance, kinetic properties, and sensitivity to various ligands (12, 13). The NR1 subunit binds to glycine and is essential for the formation of functional NMDA receptor channels, whereas the NR2 subunit binds to glutamate and quinolinic acid and modifies the channel property (12) with predominantly NR2A and NR2B in the adult rat hippocampus (14, 15). Expression patterns of the NR2 subunits are function-

[3] The abbreviations used are: NMDAR, N-methyl-D-aspartate receptor; NMDA, N-methyl-D-aspartate; DIV, day in vitro; LDH, lactate dehydrogenase; PND, postnatal day; E, embryonic day; P, postnatal day; i.c.v., intracerebroventricular; BSS, balanced salt solution; CREB, cAMP-response element-binding protein.

ally regulated with development in rodent brains (14). It has been reported that neuronal susceptibility to excitotoxicity also changes with development both *in vivo* (16) and *in vitro* (17, 18), but the underlying mechanisms are not fully known. Although the calcium influx and MAPK activations have been well documented to be highly involved in both NMDA-induced neurotoxicity and neuroprotective effects (19), the relationship between these signals and the changes of neuronal sensitivity to NMDA toxicity during development remains to be elucidated. In this study, we determine this issue in cultured hippocampal neurons and intact animals. We check the pro-survival/death roles of NMDA in different aged neurons and test the profiles of the correlative NMDA-evoked ERK1/2 and p38 MAPK activation as well as calcium influx during neuron maturation. We also investigate the subunit contributions of NR2A- and NR2B-containing NMDARs to the above effects.

EXPERIMENTAL PROCEDURES

Primary Hippocampal Neuron Culture—All animal procedures were approved by the Institutional Animal Care and Use Committee of Second Military Medical University. Procedures were designed to minimize the number of animals used and their suffering. Hippocampal neuron cultures were prepared as described previously (20). Briefly, hippocampi were dissected from embryonic day 18 (E18) Sprague-Dawley rat fetuses in ice-cold dissection solution containing sucrose/glucose/HEPES (DISGH solution: 136 mM NaCl, 5.4 mM KCl, 0.2 mM Na_2HPO_4, 2 mM KH_2PO_4, 16.7 mM glucose, 20.8 mM saccharose, 0.0012% phenol red, and 10 mM HEPES, pH 7.4). Isolated hippocampi were mechanically triturated, and then digested in solution containing 0.25% trypsin and 1 mM EDTA at 37 °C for 15 min. Single cell suspension was obtained by repeatedly passaging dissociated tissues through a fire-polished pipette in DMEM supplemented with 10% heat-inactivated FBS and horse serum. Cells were finally plated on poly-L-lysine (0.1 mg/ml)-coated 24-well plates or dishes for different experiments at optimal cell densities. The serum containing plating medium was replaced by a serum-free Neurobasal medium supplemented with 2% B27 (culture medium) within 24 h after plating. Half of the culture medium was changed every 3 days thereafter. More than 95% cells were neurons as verified by positive staining of microtubule-associated protein-2 (MAP2) against Hoechst. Neurons were used at 3, 6, 9, 12, or 15 day *in vitro* (DIV) according to different experiments.

In Vitro Neurotoxicity Assay—NMDA treatments of neurons were carried out at room temperature in modified Locke's solution (154 mM NaCl, 5.6 mM KCl, 3.6 mM NaHCO₃, 2.3 mM CaCl₂, 5.6 mM D-glucose, 10 mM HEPES, 10 μM glycine, pH 7.4) as described previously (21). Briefly, on proper *in vitro* culture days, the original culture medium was collected and replaced by Locke's solution before drug administration. Neurons were treated with various concentrations of NMDA diluted in Locke's solution or control (Locke's solution alone) for 15 min, followed by a washout with DMEM, and then returned to the original culture medium. For neuroprotection study in immature neurons, cells were incubated in DMEM without any nutrition supplement after NMDA stimulation (DMEM protocol). For high calcium assay, the concentration of CaCl₂ in Locke's

solution was adjusted to 5 mM. For NMDAR antagonist testing, neurons were preincubated with (+)-5-methyl-10,11-dihydro-5*H*-dibenzo[*a*,*d*]cyclohepten-5,10-imine maleate (MK-801, 0.3 μM), *R*-(*RS*)-α-(4-hydroxyphenyl)-β-methyl-4-(phenylmethyl)-1-piperidinepropranol (Ro25-6981, 0.5 μM) (Tocris, Cookson, Bristol, UK), or [(*R*)-[(*S*)-1-(4-bromophenyl)-ethylamino]-(2,3-dioxo-1,2,3,4-tetrahydroquinoxalin-5-yl)-methyl] phosphonic acid (NVP-AAM077, 0.5 μM) (a kind gift from Dr. Yves P. Auberson, Novartis Institutes for Biomedical Research, Basel, Switzerland) for 20 min before adding NMDA. For p38 or ERK1/2 MAPK inhibitor treatments, neurons were preincubated with SB203580 (10 μM) or PD98059 (10 μM) for 20 min before adding NMDA. After a 24-h recovery period, neuronal cell death was estimated by examination of culture morphology under phase-contrast microscopy and quantitatively assessed by measurement of the lactate dehydrogenase (LDH) released into the culture supernatant by damaged or dead cells as described previously (21). Briefly, 50 μl of cell supernatant were taken out from each treatment and subjected to LDH assay using a cytotoxicity assay kit (Promega). Neuronal cell damage was measured by the absorbance at 490 nm with a microplate reader 680 (Bio-Rad), and the relative damage intensities were calculated by normalizing to the cells with vehicle treatment (control). Results were from four independent experiments with three replicates for each data point per experiment.

Nuclear Staining with Hoechst 33342—For nuclear staining analysis of excitotoxic neuronal death, neurons subjected to excitotoxic treatment were fixed with 4% paraformaldehyde for 20 min at room temperature after a 24-h recovery period and washed with phosphate-buffered saline (PBS). They were then incubated with 2 μg/ml Hoechst 33342 at room temperature for 15 min at room temperature and washed again with PBS. Neurons were viewed under phase and fluorescence microscopy. The presence of nuclear chromatin condensation or fragmentation was examined as damaged cells, and those that showed round and uniform staining were judged as intact cells. Results were from three independent experiments. In each experiment, 20–30 randomly captured fields from each well were counted with three replicates for each treatment. About 5000 cells were counted for each data point.

Intracerebroventricular (i.c.v.) Injection of NMDA—Young adult (3 month) male Sprague-Dawley rats (250–300 g, *n* = 6) or postnatal day 12 (PND) male pups (*n* = 6) were anesthetized by vaporized ethyl ether and fixed in a stereotaxic apparatus, and a Hamilton syringe was inserted into the lateral cerebral ventricle through a drilled opening using the following coordinates: anterior-posterior = −1 mm from bregma; lateral = 1.5 mm; dorsoventral = 3.5 mm from the skull surface (22). A dose of 60 nmol of NMDA that was freshly dissolved in PBS (60 mM, 1 μl) was infused slowly (0.2 μl/min) into the right lateral ventricle. It has been estimated that the actual initial extracellular (perineuronal) concentrations of NMDA would be about 1 mM in PND12 rats under such circumstances (23). As dissolution of NMDA in a 60 mM concentration considerably decreases the pH value of its vehicle (~pH 4.0), the pH-equivalent PBS was used as a control solution. Control lesions (1 μl of PBS, pH 4.0) were performed contralaterally (left side). *In utero* microinjection of E18 rat embryo (*n* = 6) and microinjection of neonatal

P1 pups ($n = 6$) were done following the published surgical protocol (24). For easy and reasonable comparison with young adult and PND12 rats, two doses of NMDA were examined that were 30 nmol (60 mM, 0.5 μl) and 60 nmol (60 mM, 1 μl), respectively. NMDA or PBS was injected into the ventricles using a mouth-controlled pipette system with the micropipette, which was made by pulling 75-mm glass capillary microhematocrits (Drummond Scientific, Broomall, PA) using a micropipette puller P-97/IVF (Sutter Instruments, Novato, CA). We were able to inject the solution approximately into the aimed site, because the surface of the telencephalon is visible through the uterine wall of the embryo or the skull of the P1 rat, by illumination of a fiber optics light source. Neurotoxic effects of NMDA on hippocampal neurons were studied after 24 h.

Histological Procedures and Nissl Staining—For examination of neuronal damage, rats were killed 24 h after i.c.v. injection and studied by Nissl staining. Fixation of the brains was carried out under deep sodium pentobarbital anesthesia by transcardial perfusion with 350 ml (for adult and PND12 rats) or 12 ml of fixative composed of 4% paraformaldehyde in 0.1 M phosphate buffer (PB, pH 7.4), which was preceded by a short prerinse (50 ml) with ice-cold physiological saline. Brains were removed from the cranial vault and post-fixed for 2 h in the same fixative, cryoprotected by overnight storage in 30% sucrose in 0.1 M PB at 4 °C. Thereafter, brains were embedded in Paraplast, and coronal frozen sections were cut on a cryostat microtome (Leica, Germany) at a 15-μm thickness and collected in 0.01 M PBS containing 0.1% sodium azide. Sections were mounted and blotted onto slides before being processed through different baths in the following order: 100% ethyl alcohol (EtOH), 2 min; xylene, 2 min; 100% EtOH, 2 min; 70% EtOH, 2 min; distilled water, 5 min; cresyl violet, 3 min; distilled water, two dips; 70% EtOH, 5 min; 80% EtOH, 2 min; 90% EtOH, 2 min; 95% EtOH, 2 min; 100% EtOH, 5 min; xylene, 5 min; and then mounted with Permount. After 24 h, they were observed using an Olympus IX70 light microscope.

Real Time RT-PCR Analysis of NR2A and NR2B Expression—Total RNA was extracted using Takara RNAiso reagent (Takara, Japan) from neurons on different culture days. RevertAid™ first strand cDNA synthesis kits (Fermentas) were used to synthesize cDNA, and 4% of the cDNA products were used to determine the expression of NR2A and NR2B. Real time PCR assays based on SYBR Green I dye detection were carried out using the Rotor-Gen3000 system (Corbett Research, Australia) in a total volume of 25 μl of reaction mixture following the manufacturer's protocol, using the $2\times$ *Taq*PCR master mix (Qiagen) and 0.2 μM each of the following primers: rat NR2A (GenBank™ accession number NM-012573) forward, 5'-CAC-GGCGGCAATAATGGT-3', and reverse, 5'-GTCTTGGGG-GAAGCCTACAAT-3'; rat NR2B (GenBank™ accession number NM-012574) forward, 5'-ATCAGTGCTTGCTTCA-CGG-3', and reverse, 5'-GGGTTGGACTGGTTCCCTAT-3'; rat β-actin (GenBank™ accession number NM-031144) forward, 5'-GAGGCCCCTCTGAACCCTAAGG-3', and reverse, 5'-TGCGGCAGTGGCCATCTCT-3'. PCR conditions were optimized according to preliminary experiments to achieve linear relationships between initial RNA concentration and PCR products with the annealing temperature being 54 °C. The

amplification cycles were set at 40 cycles. The specificity of the primers was verified by examining the melting curve as well as subsequent sequencing of the real time RT-PCR products. As a negative control for all of the reactions, distilled water was used in place of cDNA. NR2A and NR2B mRNAs in each sample were normalized on the basis of its β-actin mRNA content. To achieve comparison between samples, the relative expression of the genes of interest was determined by using the comparative threshold cycle (Ct) method (25). Briefly, ΔCt in each group was yielded by subtracting the Ct of the actin gene from the Ct of the target gene, which yields the ΔCt in each DIV point. Then subtracting ΔCt of the control (3DIV) group from the other DIV groups obtain the $\Delta\Delta Ct$, which was entered into the equation $2^{-\Delta\Delta Ct}$ and calculated for the exponential amplification of PCR. Results were means $\pm$ S.E. from three independent experiments with three replicates for each data point.

Western Blot Analysis of NMDAR Expression and MAPK Activation—For assessment of MAPK activation in cultured hippocampal neurons, on different days *in vitro*, neurons were starved for 6 h in DMEM without any supplement and then stimulated with NMDA or not in Locke's solution for 15 min as was done in the *in vitro* excitotoxic experiments (antagonists were pretreated for 20 min). For calcium-free, high calcium, or low calcium assay, NMDA stimulation was done in the absence of the 2.3 mM $CaCl_2$ and with 5 mM EGTA or in the presence of 5 or 0.1 mM $CaCl_2$ in Locke's solution. For KCl stimulation, 50 mM KCl was added directly to the DMEM after starvation for 15 min. Cell were immediately washed twice with ice-cold 0.1 M PBS, and the cell lysates were obtained by incubating cells in ice-cold lysis buffer (0.1% SDS, 1% Igepal, 0.2 mM sodium orthovanadate, 0.2 mM phenymethylsulfonyl fluoride (PMSF)) for 20 min. To examine the activation of MAPKs *in vivo*, tissue lysates of P0 or young adult (3 month) ($n = 6$) hippocampi were obtained by RIPA (50 mM Tris-HCl, pH 7.4, 150 mM NaCl, 1% Nonidet P-40, 0.25% sodium deoxycholate, 1 mM PMSF, $1\times$ Roche Applied Science complete mini protease inhibitor) lysis buffer 30 min after i.c.v. injection of NMDA (60 mM, 1 μl) or PBS as done in *in vivo* excitotoxic experiments. For NMDAR expression, lysates of intact neurons were also collected at different days *in vitro* for NR2A and NR2B expression analysis. All lysates were cleared by centrifugation at $12,000 \times g$ for 10 min at 4 °C, and protein concentration in the supernatant was determined by the BCA protein assay (Sigma). After boiling for 5 min, 15 μg of total protein from whole-cell lysates were separated by a single layer of 15% (for p38 and ERK1/2) or double layers of 7 and 15% (for NR2A and NR2B) SDS-PAGE denaturing gel and were electrotransferred onto nitrocellulose membranes (Schleicher & Schuell). Membranes were blocked with 10% nonfat dry milk in TBST (50 mM Tris, 150 mM NaCl, and 0.1% Tween 20, v/v, pH 7.4) for 1 h, and immunoblotted with anti-phosphorylated p38, ERK1/2 (Cell signaling technology, Inc., Beverly, MA), or anti-NR2A, NR2B (Chemicon Inc.), or anti-actin (Kang Cheng Biotech., Shanghai) primary antibodies at a dilution of 1:1000 for overnight at 4 °C. Horseradish peroxidase conjugated secondary antibody was used together with ECL detection system (Pierce Biotechnology, Inc.) to detect the final signal. Membranes were stripped and reprobed with total p38 or ERK1/2 antibodies. Quantifications of MAPKs activa-

tion were done by scanning densitometry analysis on phospho-p38 and phospho-ERK1/2 against total p38 and total ERK1/2. Quantifications of NR expression were done in a similar way against actin. Scanning densities were normalized to control and expressed as relative folds of control.

Measurement of $[Ca^{2+}]_i$—Measurement of intracellular calcium concentrations ($[Ca^{2+}]_i$) was performed using the Ca^{2+}-sensitive indicator fura-2. On different culture days, neurons grown in coverslips were loaded for 1 h at 37 °C with 1 μM fura-2/AM (Dojindo, Japan) in the presence of 0.04% pluronic F-127 in Neurobasal/B27 culture medium to minimize the disturbance of neuron during handling. After fluorescence loading, the coverslips were rinsed in Mg^{2+}-free balanced salt solution (BSS in mM, 130 NaCl, 5.4 KCl, 2.0 CaCl$_2$, 5.5 glucose, 10 HEPES, and 10 μM glycine, pH 7.3) and mounted in a perfusion chamber and placed on the stage of an inverted microscope (IX70, Olympus) immediately for Ca^{2+} imaging. The neurons were then perfused at a rate of 1.5 ml/min with BSS. After recording of the basal level of $[Ca^{2+}]_i$ for 2 min, the neurons were perfused with BSS containing NMDA (100 μM) or not, and $[Ca^{2+}]_i$ was further traced for 3–5 min. For antagonist assay, neurons were perfused with BSS containing various NMDAR antagonists for 2 min and then with NMDA in the presence of antagonists for 3–5 min. For high or low calcium assay, the concentration of CaCl$_2$ in BSS was adjusted to 5 mM. For Ca^{2+} imaging, light was emitted from a 75-watt xenon arc lamp (AH2-RX, Olympus) and passed through an excitation filter set (Chroma) to generate ultraviolet monochromatic waves of 340 and 380 nm. With the aid of a computerized filter wheel (Lambda 10-2, Sutter Instruments), the cells on the coverslips were alternatively exposed to the two waves through an Olympus UApo objective. The resulting fluorescence emission from Ca^{2+}-sensitive dye was collected through a 510-nm long pass filter (Chroma) with a cooled charge-coupled device (CCD) camera (MicroMax, 5 MHz system, Princeton Instruments). All image acquisitions were computer-controlled by Metafluor Imaging program (version 4.01, Universal Imaging Corp.). Images were acquired at 3-s intervals to reduce photobleaching. $[Ca^{2+}]_i$ in each cell was expressed as F_{340}/F_{380}, which is the ratio of the fluorescence intensity at 340 nm excitation (F_{340}) to that at 380 nm excitation (F_{380}). All measurements were made at room temperature (22–25 °C).

Statistical Analysis—Comparisons between different drug treatments were performed using a one-way analysis of variance, followed by Student's *t* test. Differences were considered significant at $p < 0.05$. Data are presented as mean ± S.E. from at least three independent experiments.

RESULTS

NMDA Triggers Dramatic Neurotoxicity in Mature Hippocampal Neurons although It Is Neuroprotective for Immature Neurons—Cultured hippocampal neurons were treated with NMDA of various concentrations (0, 50, 100, 200, 500, and 1000 μM) for 15 min in Mg^{2+}-free Locke's solution followed by 24 h of recovery before LDH release was detected. As shown in Fig. 1*B*, 3- and 6DIV neurons (immature neurons) were resistant to and even to some extent favored the NMDA stimulation as the LDH release of NMDA treatment groups seemed below the

control groups. On the contrary, in the case of 9- and 12DIV neurons (mature neurons), NMDA triggered a significant increase of LDH release into the cultured medium. This increase could be completely blocked by 0.3 μM MK-801 (Fig. 1*C*), a noncompetitive NMDAR antagonist, which suggested a direct neurotoxicity evoked by the overactivation of NMDARs in our system. Consistent with the result of LDH release assay, Hoechst 33342 staining demonstrated the significant increase of nuclei chromatin condensation after treatment with 100 μM NMDA in 9- and 12DIV neurons but not in 3- and 6DIV neurons (Fig. 1, *A* and *D*). To verify if NMDA is neuroprotective for immature neurons, we further introduced a "DMEM protocol" as described under "Experimental Procedures" to make a considerable basal cell death level in the control group. Consistent to our hypothesis, it is found that NMDA treatment dramatically decreased the LDH release and nuclei condensation as compared with control in 3- and 6DIV neurons (Fig. 1, *E–G*), indicating a neuroprotective role of NMDA in those immature neurons.

NMDA Elicits Significant Neuronal Death in Hippocampi of Adult and Young Rats but Not of Embryonic and Newborn Rats—To determine whether similar developmental changes of NMDA neurotoxicity also happens concurrently *in vivo*, the i.c.v. injection method was introduced. NMDA was injected into the right lateral ventricle of E18, P1, PND12, and young adult rats. Nissl staining showed that in hippocampi of PND12 and young adult rats, a single injection of NMDA (60-nmol dose) resulted in dramatic loss of neurons in the hippocampus as detected 24 h later. However, the same dose of NMDA failed to trigger any significant neuronal death in E18 and P1 rats (Fig. 2).

Expression of NR2A and NR2B Increases Strikingly in Cultured Hippocampal Neuron during Maturation—We used both real time RT-PCR and Western blot analysis to figure out whether the developmental changes in NMDA neurotoxicity are accompanied by changes of NMDA receptor expression in hippocampal neurons during maturation. It was revealed that the expression of NR2A and NR2B increased dramatically during development in both mRNA and protein levels, with the NR2B maximized at about 9DIV and slowly came down after 12DIV (Fig. 3, *A* and *B*), whereas the NR2A continued to increase in the time frame we examined (Fig. 3, *A* and *C*). Notably, although the protein of NR2B is expressed as early as in 3DIV neurons, the protein of NR2A is hardly detectable in 3DIV neurons and only began to appear at 6DIV neurons (Fig. 3, *B* and *C*). Moreover, the result of real time RT-PCR also suggested that the overall abundance of NR2B was much higher than NR2A during the whole development period examined as the *Ct* value of NR2B is much smaller than that of NR2A, but the relative ratio of 2B/2A kept decreasing (Fig. 3*A*).

NR2B-containing NMDARs Mediate Both NMDA-induced Neurotoxicity in Mature Neurons and Neuroprotection in Immature Neurons—To find out which subtype of NMDARs is attributable to the NMDA neurotoxicity in mature neurons, we took advantage of the subunit-specific NMDAR antagonist NVP-AAM077, which preferentially inhibits NR2A-containing receptors at low concentrations of 0.4–1 μM (26–30), and Ro-6981, which specifically blocks NR2B-containing receptors (30, 31). At 12DIV, neurons were subjected to NMDA (100 μM)
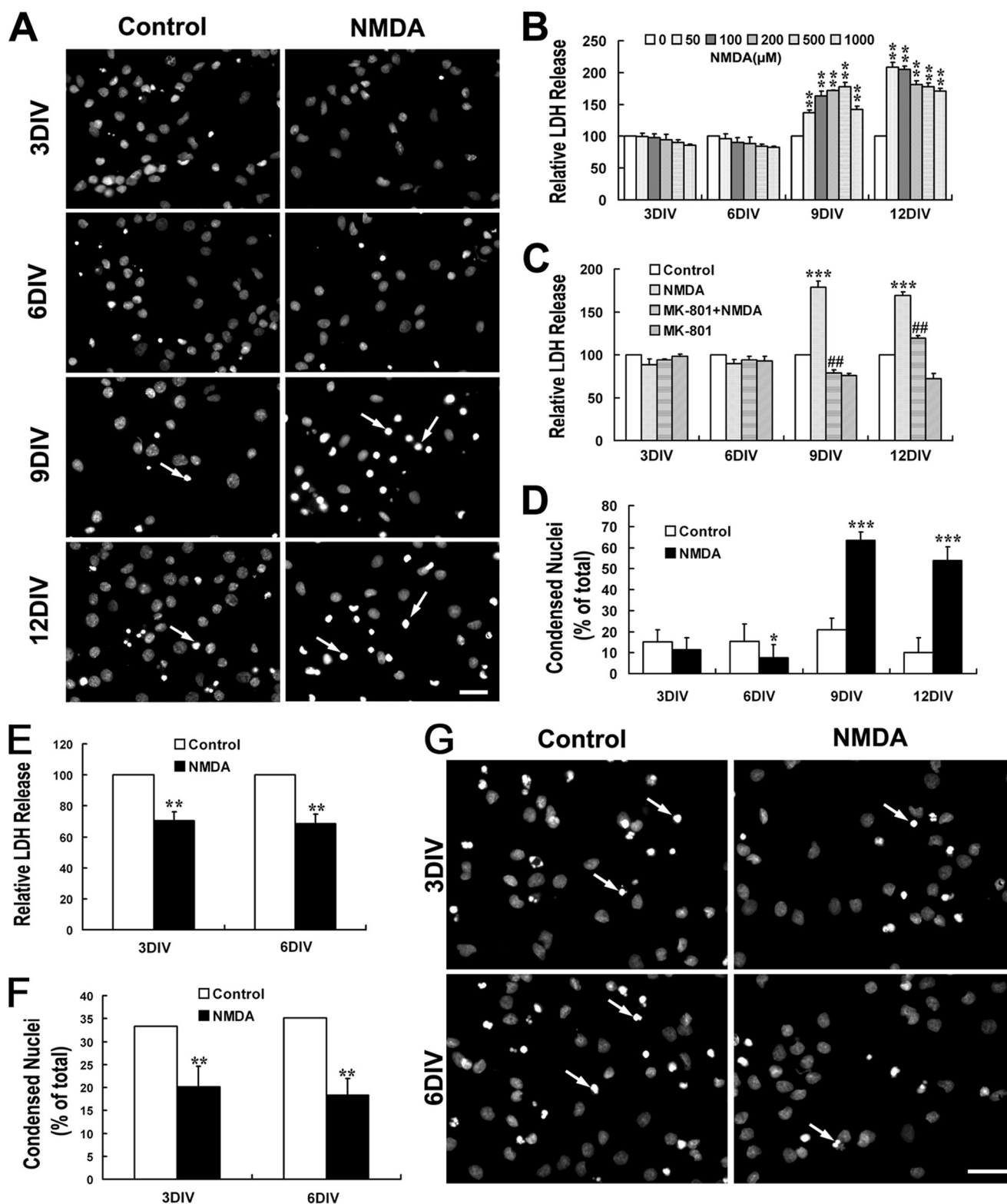
FIGURE 1. **NMDA triggers dramatic neurotoxicity in mature hippocampal neurons although it is neuroprotective for immature neuron.** At different DIV, cultured hippocampal neurons were treated with or without NMDA (100 μM) for 15 min in modified Locke's solution and washed three times with DMEM and then incubated with the original culture medium. LDH release measurements and Hoechst staining were carried out 24 h later. NMDA neurotoxicity increased significantly during neuron maturation (*A–D*). *A,* representative images of Hoechst staining showing the condensed nuclei (*arrow*) after treatment with NMDA (100 μM) or not. *B,* NMDA-induced neuronal release of LDH. **, $p < 0.01$ *versus* control (*0*). *C* and *D,* effect of MK-801 on NMDA-induced LDH release (*C*) and nuclei condensation (*D*). *, $p < 0.05$; ***, $p < 0.001$ *versus* control; ##, $p < 0.01$ *versus* NMDA. NMDA is neuroprotective against tropic deprivation in 3- and 6DIV immature neurons (*E–G*). Neurons were incubated in DMEM without any nutrition supplement after NMDA challenge or not (*DMEM protocol*). Considerable cell death could be seen in the control group. *E* and *F,* NMDA-induced neuronal of LDH release (*E*) and nuclei condensation (*F*). **, $p < 0.05$ *versus* control. *G,* representative images of Hoechst staining showing the condensed nuclei (*arrow*) in groups treated with NMDA (100 μM) or not. *Bar,* 20 μm.
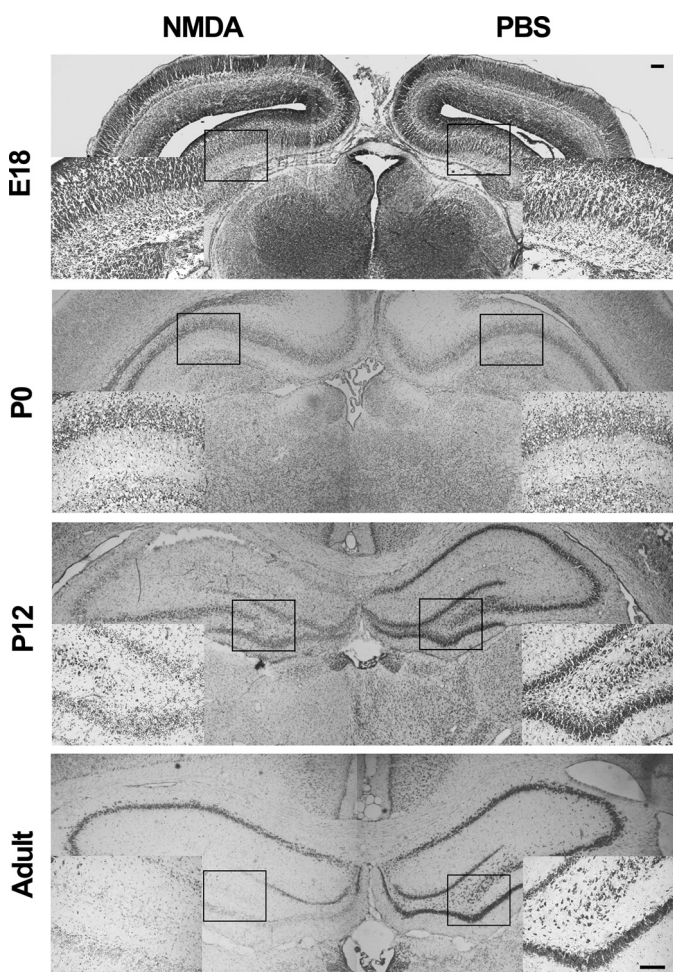
FIGURE 2. **NMDA elicits significant neuronal death in hippocampus of adult and young rats but not of embryonic and newborn rats.** Rats ($n = 6$) of indicated age were subjected to i.c.v. injection of NMDA (60 mM, 1 μl) in one side and PBS in the other side and killed after 24 h. Sections were Nissl-stained. Representative images showing the loss of Nissl stain in hippocampus of adult (3 month) and PND12 rats but not in those of E18 and P0 rats, $n = 3$. *Boxed regions* are amplified and inserted at the *bottom left* or *bottom right*. *Bar*, 100 μm.

treatment in the absence or presence of proper antagonists. As showed in Fig. 4, based on LDH release assay and Hoechst staining, it was found that the NR2B-specific antagonist Ro-6981 (0.5 μM) was as potent as MK-801 (0.3 μM), which is a noncompetitive antagonist for NMDARs, to completely block the NMDA-induced neuronal death, whereas the NR2A-specific antagonist NVP-AAM077 (0.5 μM) failed to block the neurotoxicity, suggesting a dominant role of the NR2B-containing NMDARs in mediation of the NMDA neurotoxicity in mature hippocampal neurons. Interestingly, there was a slight but statistically significant increase of NMDA-induced neuronal damage in the presence of NVP-AAM077 compared with NMDA treatment alone (Fig. 4, *B* and *C*), which indicated a neuroprotective role of NR2A-containing NMDARs in the mature neurons.

We also tested the subunit contribution of NMDARs in the neuroprotective role of NMDA in immature neurons. As shown in Fig. 4, *D* and *E*, it was demonstrated that Ro-6981 could be as effective as MK-801 at blocking the neuroprotective effect of NMDA in 3DIV neurons, whereas NVP-AAM077

failed to achieve any effects, suggesting that the neuroprotective role of NMDA in immature neurons was also mediated by NR2B-containing NMDARs.

NMDA-induced Neurotoxicity in Mature Neuron Is p38 MAPK Pathway-dependent although Neuroprotection in Immature Neuron Is ERK1/2-dependent—It is well known that ERK1/2 and p38 MAPK are intracellular signal molecules that are highly involved in the control of neuronal survival/death and can be regulated by NMDARs (19, 32, 33). We next studied the role of these MAPKs in NMDA-induced neurotoxicity in 12DIV neurons as well as the neuroprotection in 3DIV neurons. The result showed that NMDA neurotoxicity in 12DIV neurons could be blocked by p38 inhibitor SB203580 but not by ERK inhibitor PD98059 (Fig. 5, *A–C*). On the contrary, the NMDA-induced neuroprotection in 3DIV neurons could be blocked by PD98059 but not SB203580 (Fig. 5, *D* and *E*). This result implicates that the NMDA-induced neurotoxicity in mature neurons is p38 MAPK pathway-dependent, whereas the neuroprotection in immature neuron is ERK1/2-dependent. Interestingly, there was a slight but statistically significant increase of NMDA-induced neuronal damage in the presence of PD98059 in 12DIV neurons compared with NMDA treatment alone (Fig. 5*C*), which implied a neuroprotective role of ERK1/2 signaling in the mature neurons.

NMDA Prefers to Activate p38 MAPK in Mature Neuron although It Favors ERK1/2 Activation in Immature Neurons—Because it was shown that the p38 MAPK and ERK1/2 have mediated the neurotoxic or neuroprotective effect in mature and immature neurons, respectively, we wondered if the activation of profiles of p38 and ERK1/2 by NMDA also changed with development. By Western blot analysis, it was found that NMDA triggered dramatic p38 activation in 9- and 12DIV but not in 3- and 6DIV neurons (Fig. 6). This result implies that the coupling of NMDA receptors to the p38 MAPK pathway establishes as a function of neuronal development. Taking the blockage effect of p38 inhibitor on the NMDA neurotoxicity in 12DIV neurons (Fig. 5, *B* and *C*) together, it is suggested that the dramatically increased NMDA neurotoxicity in mature neurons can be attributed to the striking p38 MAPK activation induced by NMDA.

We also examined the issue of ERK1/2, whose activation is believed to be neuroprotective in many situations (33). Interestingly, it was found that NMDA elicited a strong activation of ERK1/2 in 3- and 6DIV neurons, whereas this activation is rather weak in 9- and 12DIV neurons (Fig. 6), which was in direct contrast to the profile of p38 activation. The significant attenuation of NMDA-induced ERK1/2 activation in mature neurons suggests that there might be a dramatic change in the way that NMDA receptors link to and control the ERK1/2 pathway with development. Taken together, the blockage effect of ERK1/2 inhibitor on NMDA induced neuroprotection in 3DIV neurons (Fig. 5, *D* and *E*) and the slightly enhanced neuronal damage in the presence of this inhibitor in 12DIV neurons (Fig. 5*C*), and it is supposed that although the strong activation of ERK1/2 confers the neuroprotective role of NMDA in the immature neurons, this protective effect would be significantly decreased in the mature neurons due to the sharp weakening of NMDA-induced ERK1/2 activation. This might further increase the susceptibility of mature neurons to the NMDA neurotoxicity in addition to the p38 activation. Thus, the dra-
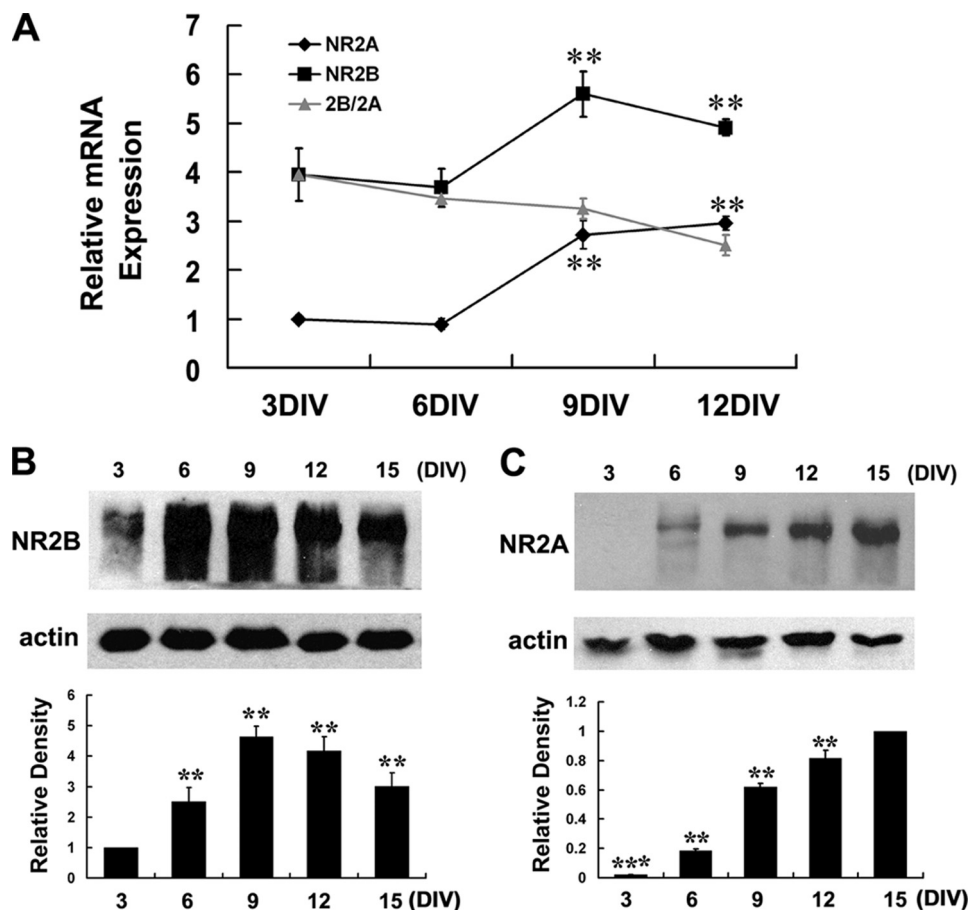
FIGURE 3. **Expression of NR2A and NR2B increases strikingly in cultured hippocampal neurons during maturation.** *A,* real time RT-PCR analysis of NR2A and NR2B expression. Relative mRNA abundances were normalized to the NR2A mRNA of 3DIV neurons. **, $p < 0.01$ *versus* 3DIV. Note that the overall abundance of NR2B is much higher than NR2A during the whole examined period, but the relative ratio of 2B/2A kept decreasing. *B* and *C,* Western blot analysis of NR2B and NR2A protein expression. Scanning densitometry was quantified and normalized to 3DIV (*B*) or 15DIV (*C*) on the same Western blots. **, $p < 0.01$ *versus* 3DIV (*B*); **, $p < 0.01$; ***, $p < 0.001$, *versus* 15DIV (*C*). Representative blots were showed from three independent experiments.

matic changes in NMDA neurotoxicity during maturation might be reasonably attributed to the switch of NMDAR-favorite intracellular signaling from the pro-survival ERK1/2 pathway to the pro-death p38 MAPK pathway with development.

NMDA Prefers to Activate p38 MAPK in Adult Rat Hippocampus although It Favors ERK1/2 Activation in P0 Rat Hippocampus—We used i.c.v. injection of NMDA to test if a similar change of NMDA-induced ERK1/2 and p38 activation also happens concurrently *in vivo* with development. It was found that NMDA triggered strong ERK1/2 activation in P0 rat hippocampus, although this was very weak in the young adult rat (Fig. 7, *A* and *B*). On the contrary, there was dramatic activation of p38 MAPK in the young adult rat hippocampus but not in P0 rat in response to NMDA stimulation (Fig. 7, *A* and *B*). This result was consistent with the switch of the NMDAR-favorite signal pathways from ERK1/2 to p38 MAPK in the cultured hippocampal neurons during maturation, and it indicated that such a switch also exists *in vivo*, which might be responsible for the increased susceptibility of rat hippocampus to NMDA neurotoxicity with development.

One may argue that this switch could be a reflection of nonspecific global changes of intracellular signal pathways to extracellular stimulations during neuronal development. To rule out this possibility, we carried out a comparative study of the

MAPKs activation induced by NMDA and KCl in both mature and immature neurons. We used KCl because the membrane depolarization induced by high KCl has been well documented to activate MAPKs in neurons (34). The result showed that although NMDA elicited dramatic activation of ERK1/2 only in 3DIV neurons and p38 only in 12DIV neurons, KCl depolarization triggered significant activation of ERK1/2 and p38 in both 3- and 12DIV neurons (Fig. 7, *C* and *D*). Thus, it is likely that the switch of the NMDAR-favorite signal pathways from ERK1/2 to p38 MAPK in hippocampal neuron is specifically occurred during maturation.

NR2B-containing NMDARs Mediate Both p38 MAPK Activation in Mature Neuron and ERK1/2 Activation in Immature Neuron—Because it was shown that the NMDA-induced neurotoxicity in mature neurons was NR2B-containing NMDARs and p38 pathway-dependent, although the neuroprotection in immature neurons was NR2B and ERK1/2 pathway-dependent (Figs. 4 and 5), we asked whether the activation of ERK1/2 and p38 was also mediated specifically by NR2B-containing NMDARs. It was revealed that the both the NMDA-evoked p38 activation in 12DIV neurons and ERK1/2 activation in 3DIV neurons were blocked by Ro-6981 and MK-801 but not by NVP-AAM077 (Fig. 8), indicating that NR2B-containing NMDA receptors mediate both the pro-death p38 MAPK path-
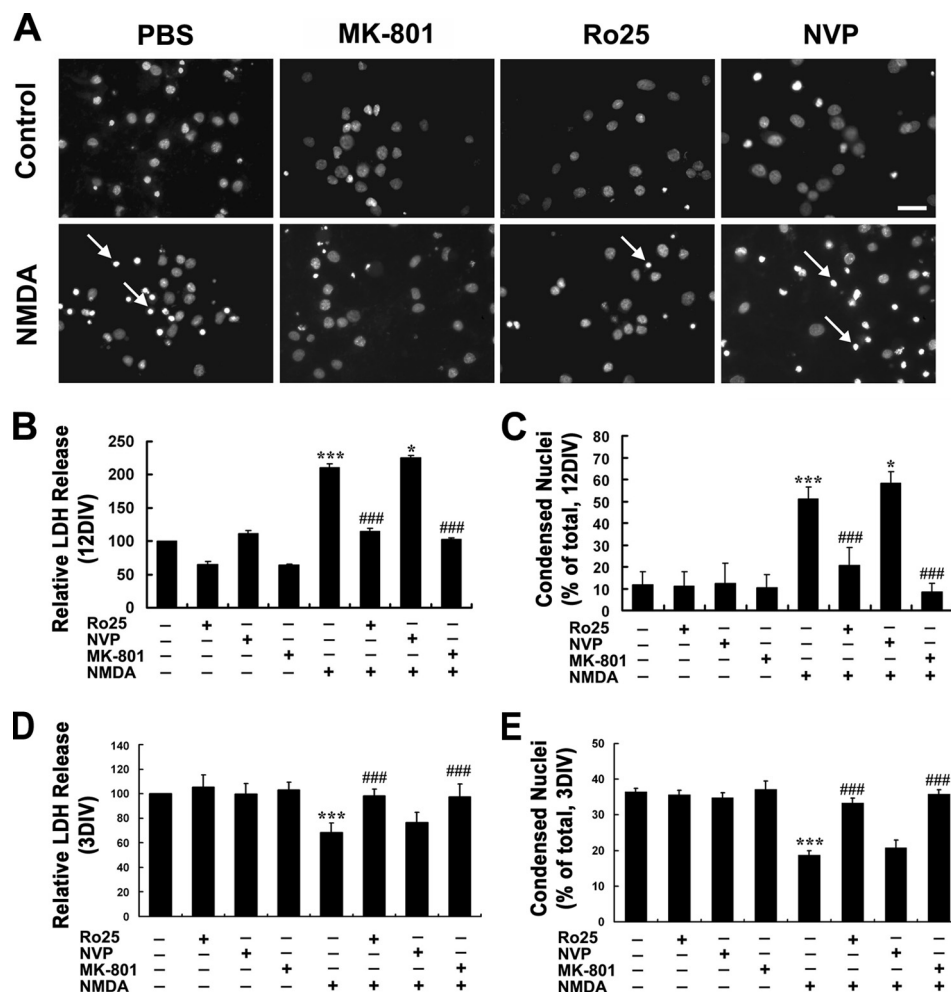
FIGURE 4. **NR2B-containing NMDARs mediate both NMDA-induced neurotoxicity in mature neuron and neuroprotection in immature neuron.** At 12- or 3DIV, neurons were pretreated with Ro-6981 (*Ro25*, 0.5 μM), NVP-AMM077 (*NVP*, 0.5 μM), MK-801 (0.3 μM), or PBS for 20 min followed by treatment with or without NMDA (100 μM) for 15 min in modified Locke's solution and washed three times with DMEM and then incubated with original culture medium (*A–C*) or DMEM (*D* and *E*). LDH release measurement and Hoechst staining was conducted 24 h later. *A,* typical images showing the nuclear condensation (*arrow*) under various treatment conditions as indicated. *B* and *D,* LDH release assay. *C* and *E,* Hoechst staining. ***, *p* < 0.001 *versus* sham treatment; *, *p* < 0.05, ###, *p* < 0.001 *versus* NMDA alone. Note the significantly decreased neuronal death in 12DIV neuron in the presence of Ro-6981 and the slight increase of in the presence of NVP-AMM077, which is more obvious in 3DIV neuron. *Bar,* 20 μm.

way in mature neurons and the pro-survival ERK1/2 pathway in immature neurons, as shown in a schematic diagram (Fig. 11). Interestingly, it was also found that the much weaker activation of ERK1/2 in 12DIV neurons (also see in Figs. 6 and 7) was blocked by NVP-AAM077 but not by Ro-6981. On the contrary, this activation was even enhanced in the presence of Ro-6981 (Fig. 8, *B* and *D*). Taken together, the enhanced neuronal damage in the presence of NR2A-specific antagonist (Fig. 4*C*) or ERK1/2 inhibitor in 12DIV neurons (Fig. 5*C*), it is supposed that there also exists a pro-survival ERK1/2 signaling pathway that is mediated by the NR2A-containing NMDARs in the mature neurons, and this pathway could be inhibited by NR2B signaling (as shown in Fig. 11). In fact, such a pro-survival NR2A-ERK1/2 pathway has also been previously reported in 10DIV neurons in the same system (21).

NMDA Triggers Similar Calcium Influx Both in Mature and Immature Neurons, Although the Basal [Ca^{2+}]$_i$ Level Elevates with Development—Calcium signal is extremely important for the various physiological effects of NMDARs. Extracellular Ca^{2+} influx and the consequent intracellular Ca^{2+} overload

have been suggested to be the major pathological disturbances during NMDA neurotoxicity (10, 35–37). Therefore, we checked the pattern of the NMDA-induced [Ca^{2+}]$_i$ increase in hippocampal neurons with development. It was found that despite the absence of NMDA-induced neurotoxicity in 3- and 6DIV immature neurons, the NMDA-induced increase of [Ca^{2+}]$_i$ can be detected in cultured neurons of all ages (Fig. 9, *A–C*). Interestingly, the amplitudes of Ca^{2+} influx were similar between the responsive neurons (cell that showed Δratio ≥0.1) of different developmental stages (Fig. 9*C*), whereas the basal level of [Ca^{2+}]$_i$ in hippocampal neurons showed a continuous increase with the culture age (Fig. 9*D*). Moreover, antagonist assays showed that the NMDA-induced [Ca^{2+}]$_i$ increase in 3DIV neurons could be completely blocked by MK-801 and Ro-6981 but not affected by NVP-AAM077, although in 12DIV neurons, it was blocked completely only by MK-801 and partially by both Ro-6981 and NVP-AAM077 (Fig. 9*E*). This result suggests that although it is predominantly NR2B-containing NMDARs that function in immature neurons, both NR2B and NR2A-containing NMDARs are functional in the mature neu-
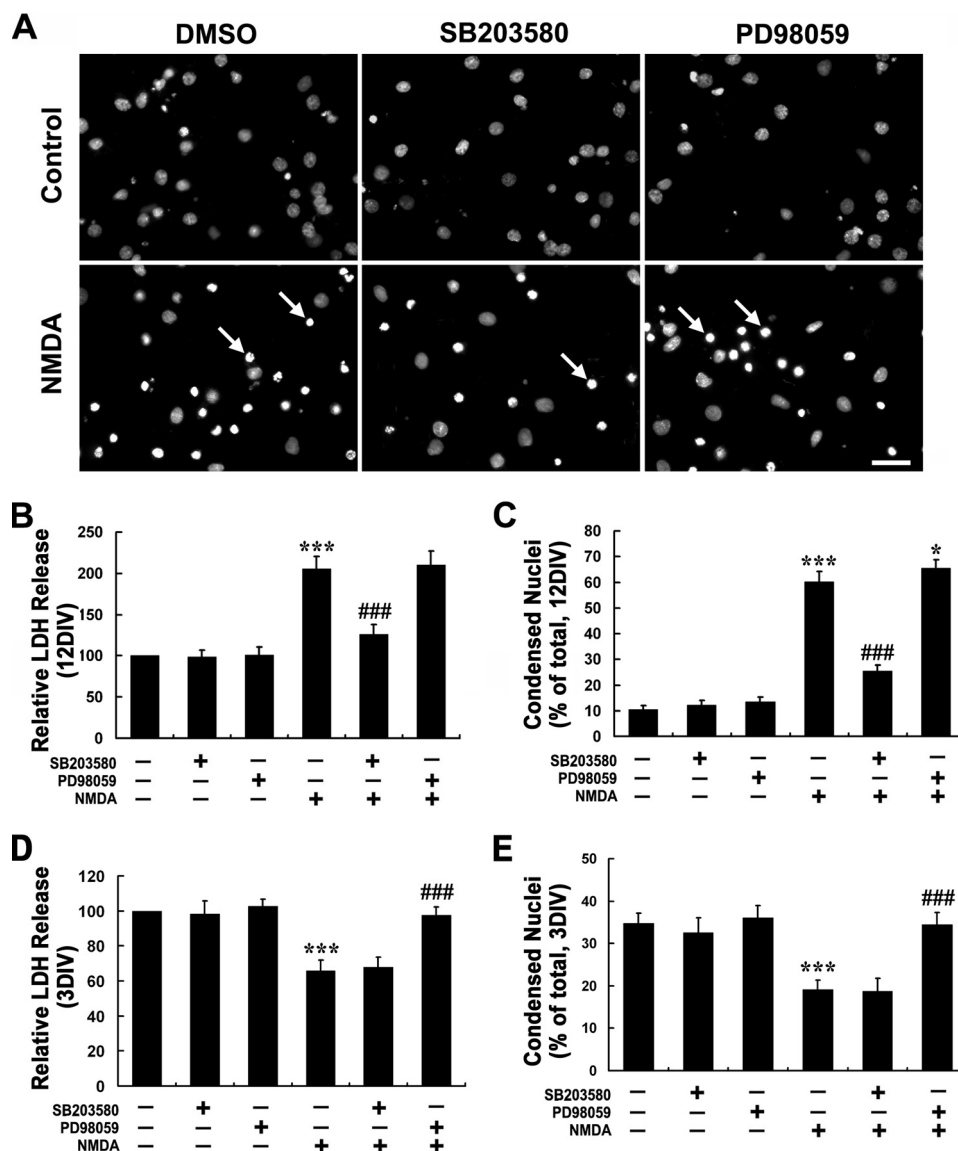
FIGURE 5. **NMDA-induced neurotoxicity in mature neuron is p38 MAPK pathway-dependent, whereas neuroprotection in immature neuron is ERK1/2-dependent.** At 12 or 3DIV, neurons were pretreated with p38 MAPK-specific inhibitor SB203580 (10 μM), ERK1/2-specific inhibitor PD98059 (10 μM), or DMSO for 20 min followed by treatment with or without NMDA (100 μM) for 15 min in modified Locke's solution and washed three times with DMEM and then incubated with original culture medium (*A–C*) or DMEM (*D* and *E*). LDH release measurement and Hoechst staining were conducted 24 h later. *A*, typical images showing the nuclear condensation (*arrow*) under various treatment conditions as indicated. *B* and *D*, LDH release assay; *C* and *E*, Hoechst staining. ***, $p < 0.001$ *versus* sham treatment; *, $p < 0.05$; ###, $p < 0.001$ *versus* NMDA alone. Note the significantly decreased neuronal death in 12DIV neuron in the presence of SB203580 and the slight increase f in the presence of PD98059, which is more obvious in 3DIV neuron. *Bar*, 20 μm.

ron, which was in consistent with the expression patterns of the NR2B and NR2A during development.

NMDA Neurotoxicity, but Not NMDA-induced ERK1/2 and p38 MAPK Activation Changes with Extracellular Calcium Level—We next asked what was the relationship was between NMDA-induced calcium influx, activation of MAPKs, and the ultimately pro-neuronal survival/death effect during development. We carried out a calcium-free assay in the presence of 5 mM EGTA. It was found that in the absence of extracellular calcium, the NMDA-induced calcium influx was completely abrogated in both 3- and 12DIV neurons (data not shown), and its pro-survival or pro-death effects in these neurons were also abolished accordingly (Fig. 10*A*). Moreover, the NMDA-induced ERK1/2 activation in 3DIV neurons and p38 activation in 12DIV neurons was also eliminated in the calcium-free conditions.

Thus, it is indicated that the above effects of NMDA in both immature and mature neurons were all calcium-dependent.

To further see if the elevated basal $[Ca^{2+}]_i$ was responsible for the increased NMDA neurotoxicity and the switch of NMDAR-favored signaling pathways in hippocampal neurons during maturation, we conducted high and low extracellular calcium assays in 3- and 12DIV neurons by adjusting the concentration of $CaCl_2$ to 5 and 0.1 mM, respectively, in Locke's and BSS solution. It was found that in the presence of 5 mM $CaCl_2$, 3DIV neurons showed significantly increased basal $[Ca^{2+}]_i$ than in normal conditions (2 mM $CaCl_2$), which was at a level comparable with that of 12DIV neurons in normal conditions (Fig. 10*B*). At the same time, NMDA triggered more intensive calcium influx to reach a similar $[Ca^{2+}]_i$ level as NMDA did in 12DIV neurons in normal conditions (Fig. 10*B*). Interestingly,
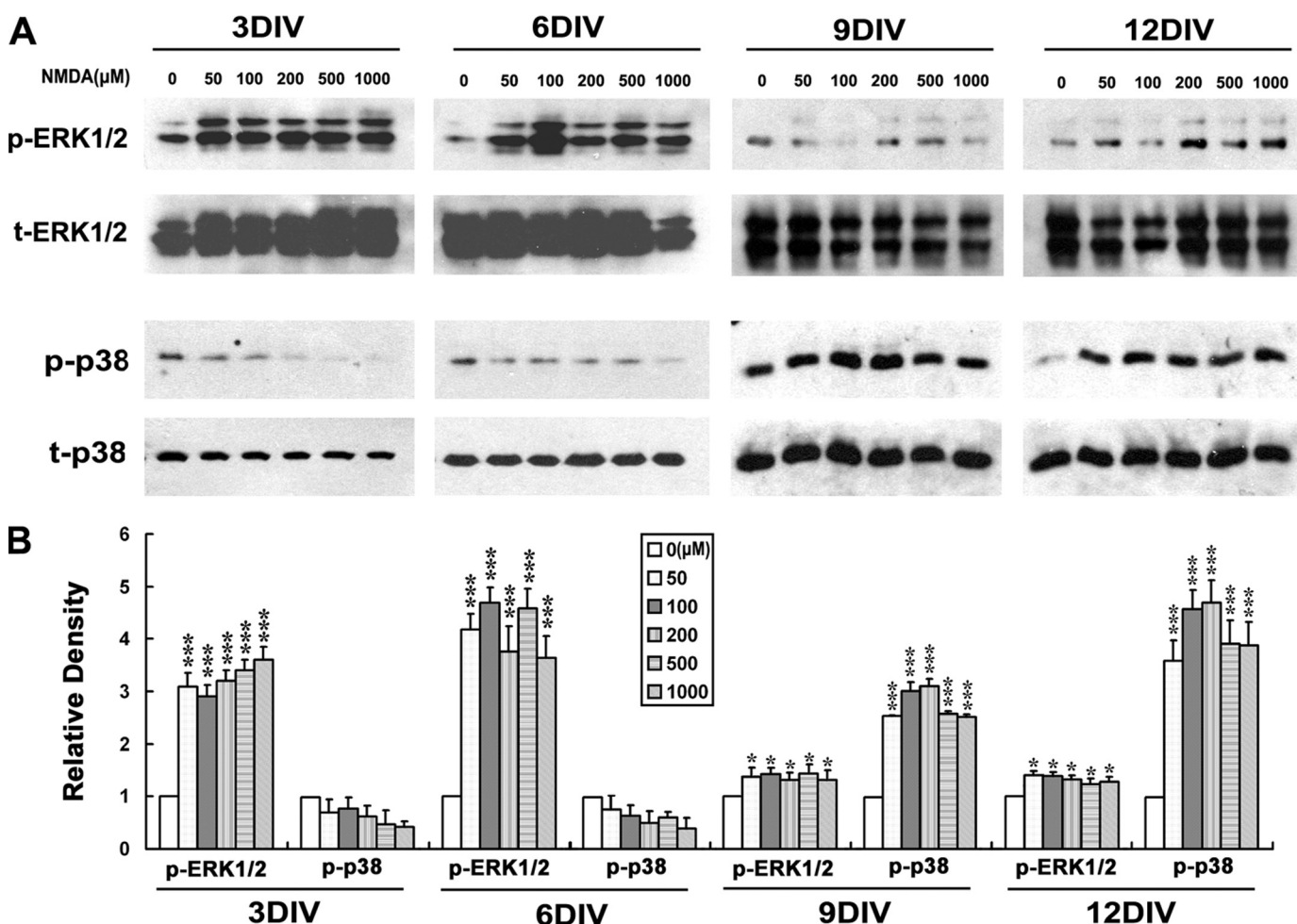
FIGURE 6. **NMDA prefers to activate p38 MAPK in mature neurons, whereas it favors ERK1/2 activation in immature neurons.** On different days *in vitro*, neurons were starved for 6 h in DMEM without any supplement and then stimulated with the indicated concentrations of NMDA or not in Locke's solution for 15 min. Whole-cell lysates were harvested, and immunoblotting was done by using of anti-phosphorylated p38 or ERK1/2 antibodies (*p-p38, t-ERK1/2*) and anti-total p38 or ERK1/2 (*t-p38, p-ERK1/2*) antibodies, with the latter serving as an internal control for protein loading to assess the activation level of p38 and ERK1/2. *A*, representative blots from 4 independent experiments. *B*, scanning densitometry was quantified and normalized to sham treatment values on the same blots. *, $p < 0.05$; ***, $p < 0.001$ *versus* control (*0*). Note the dramatic activation of p38 in 9- and 12DIV neurons but not in 3- and 6DIV neurons, and the strong activation of ERK1/2 in 3- and 6DIV neurons, which becomes rather weak in 9- and 12DIV neurons.

3DIV neurons became susceptible to NMDA neurotoxicity at high extracellular calcium conditions, although they were resistant at normal conditions (Fig. 10*D*). However, when 12DIV neurons were treated in the presence of 0.1 mM CaCl₂, the basal $[Ca^{2+}]_i$ decreased dramatically to a level comparable with that of 3DIV neurons in normal conditions (Fig. 10*B*), and the NMDA-induced neurotoxicity was also significantly decreased (Fig. 10*D*). Despite the significant changes of basal $[Ca^{2+}]_i$ and the NMDA-induced calcium influx and neurotoxicity with the changes of extracellular calcium concentrations in 3- and 12DIV neurons, however, there was no alteration in the patterns of NMDA-induced ERK1/2 and p38 MAPK activation. NMDA preferentially activated ERK1/2 in 3DIV neurons at either normal or high calcium conditions, and it favored p38 activation in 12DIV neurons at either normal or low calcium conditions (Fig. 10*C*). These results indicate that the elevated basal $[Ca^{2+}]_i$ is at least partially responsible for the developmentally increased NMDA neurotoxicity, although it seems not to contribute to the switch of NMDAR-favorite signaling pathways from ERK1/2 to p38 MAPK in hippocampal neurons during maturation.

DISCUSSION

The six principal findings of this study are as follows: 1) NMDA triggered dramatic neurotoxicity in mature hippocampal neuron but was protective in immature neuron. 2) Expression of both NR2A and NR2B NMDAR subunits were up-regulated significantly during neuron maturation, with NR2B preceding NR2A. 3) NR2B-containing NMDAR-mediated p38 MAPK activation was responsible for the NMDA neurotoxicity in the mature neuron, whereas NR2B-containing NMDAR-mediated ERK1/2 activation was responsible for the NMDA neuroprotection in immature neuron. 4) NMDAR stimulation preferred to activate p38 MAPK in the mature neuron, although it favored ERK1/2 activation in the immature neuron. 5) Both mature and immature neurons showed a similar response pattern of $[Ca^{2+}]_i$ increase to NMDA stimulation, whereas the basal levels of $[Ca^{2+}]_i$ kept elevating during neuron maturation. 6) NMDA neurotoxicity changed with extracellular calcium level, although the NMDA-induced ERK1/2 and p38 MAPK activation did not.
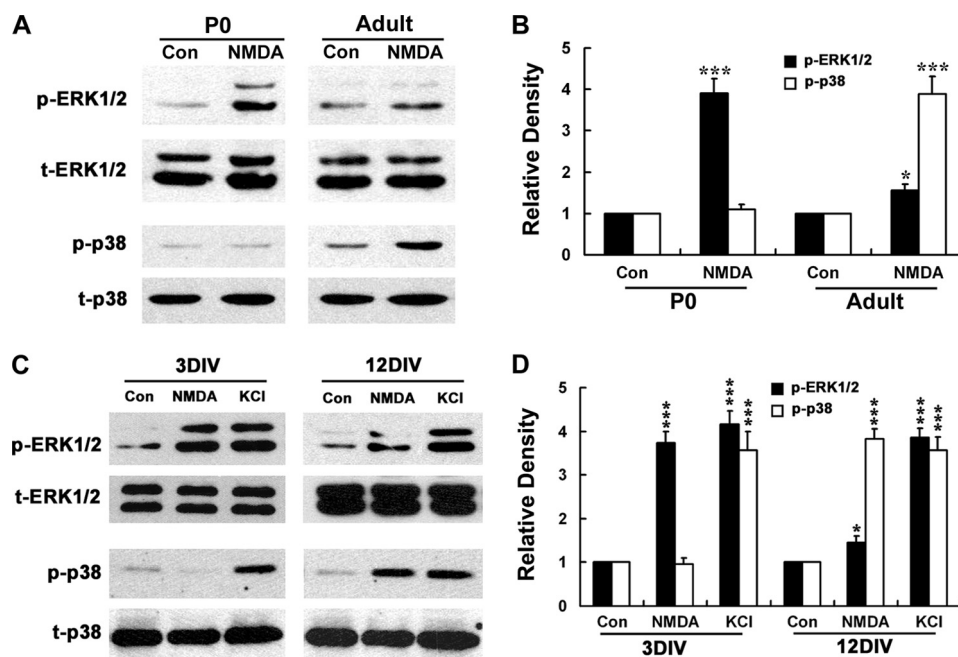
FIGURE 7. **NMDA prefers to activate p38 MAPK in adult rat hippocampus, although it favors ERK1/2 activation in P0 rat hippocampus.** *A* and *B,* NMDA (60 mM, 1 μl) or PBS (control) was administered to adult or P0 rat ($n = 6$) by i.c.v. injection. After 30 min, hippocampi were dissociated and tissue lysates were harvested. *C* and *D,* activation patterns of ERK1/2 and p38 triggered by high KCl did not change with development as those triggered by NMDA. On 3 or 12DIV, neurons were starved for 6 h in DMEM without any supplement and then stimulated with NMDA (100 μM) or not in Locke's solution for 15 min, and whole-cell lysates were harvested. Immunoblotting was done by using of anti-phosphorylated p38 or ERK1/2 antibodies (*p-p38, p-ERK1/2*) and anti-total p38 or ERK1/2 (*t-p38, t-ERK1/2*) antibodies, with the latter serving as an internal control (*Con*) for protein loading to assess the activation level of p38 and ERK1/2. *A* and *C,* representative blots from three independent experiments. *B* and *D,* scanning densitometry was quantified and normalized to sham treatment value on the same blots. *, $p < 0.05$; ***, $p < 0.001$ *versus* control (*Con*). Note that under NMDA stimulation, dramatic activation of p38 appears in adult rat hippocampus and 12DIV neurons but not in P0 rat hippocampus, whereas strong activation of ERK1/2 exhibits only in P0 rat hippocampus and 3DIV neurons, and it becomes rather weak in adult rat hippocampus. Also note that there are no significant differences in high KCl-induced ERK1/2 and p38 MAPK activation between 3- and 12DIV neurons.

Change of NMDA Neurotoxicity during Development

It has been well reported that the neuronal vulnerability to excitotoxicity can be developmentally regulated. However, the underlying mechanism remains unclear, and the definite pattern of the regulation has been controversial. Results from different models seemed not consistent with each other. Most data suggested that neuronal vulnerability to excitotoxicity increased with development. For example, *in vivo* studies by injection of glutamate into the hippocampi of relatively mature rats (P30–P60) resulted in significantly larger lesions than did in more juvenile rats (P10–P20) (16). By *in vitro* studies, susceptibility to glutamate- or NMDA-induced cell death was also shown to increase during maturation in cultured neurons from rat forebrain (36), cortex (38), cerebellum (39, 40), and hippocampus (41), as well as from murine cortex (18, 39, 42). However, there were also studies that showed decreased neuronal sensitivity to excitotoxicity with development. By direct injection of NMDA into the striatum and hippocampus, McDonald *et al.* (43) detected much weaker neurotoxicity in adult rats than in P7 neonatal rats. In acute hippocampal slices, Zhou and Baudry (17) demonstrated substantial NMDA-induced LDH release and propidium iodide uptake in slices from P7 new natal rats but not in those from adult ones. Additionally, it has also been reported that hippocampal slices cultures of different ages were equally sensitive to NMDA neurotoxicity (44). In this study, we showed that neuronal susceptibility to NMDA neurotoxicity increased with development both in hippocampal

neuron cultures and in rat hippocampus. In the culture system, whereas NMDA challenge evoked significant neuronal death in mature neuron of 9- and 12DIV (Fig. 1, *A–D*), immature hippocampal neuron of 3- and 6DIV were completely resistant to the same concentrations (50–1000 μM) of NMDA stimulations. Surprisingly, NMDA stimulation even showed significant pro-survival effects on immature neurons against trophic deprivation insult (Fig. 1, *E–G*). Consistent with the *in vitro* result, *in vivo* i.c.v. injection of NMDA elicited dramatic neuronal loss in hippocampi of young adult and P12 rats but not in E18 and P1 rats (Fig. 2). Thus, in agreement with the most popular view that NMDA neurotoxicity increases with development, our results further extend it by demonstrating that NMDA is not toxic but is instead neuroprotective to immature neuron, which indicates an opposite effects of NMDA on hippocampal neuronal survival depending on the developmental stages.

Mechanisms for Developmental Changes in NMDA Neurotoxicity

Lack of Functional NMDARs in Immature Neurons—The mechanism underlying the increased neuronal vulnerability to NMDA toxicity during development is still not fully known. It has been generally attributed to the up-regulated NMDA receptor expression, *i.e.* the resistance in immature neurons is due to the lack of NMDA receptor. As shown in the current system, NR2B and NR2A expression both increased dramatically over time in culture. Specifically, the mRNA and protein of
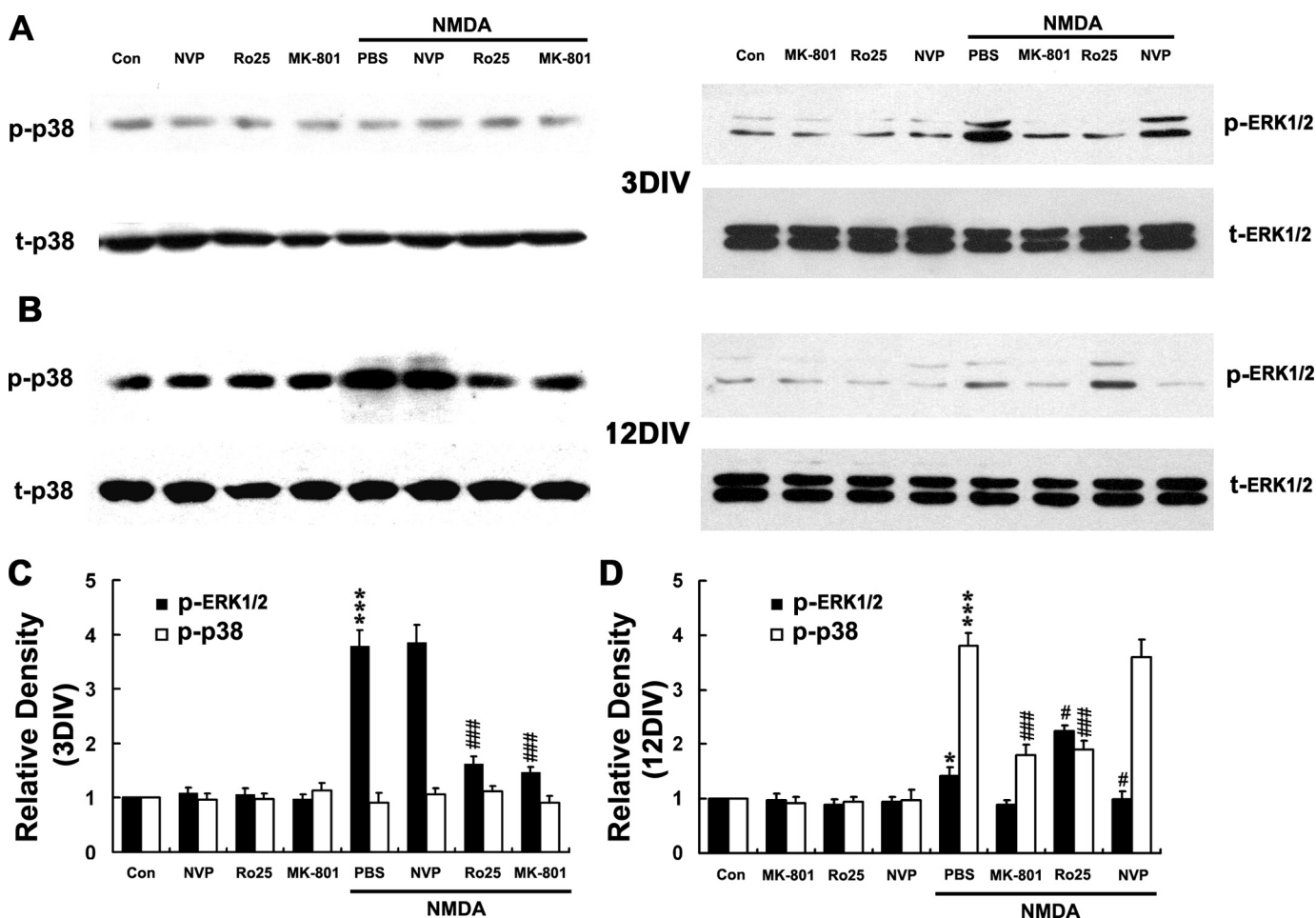
FIGURE 8. **NR2B-containing NMDARs mediate both p38 MAPK activation in mature neuron and ERK1/2 activation in immature neuron.** At 3 or 12DIV, neurons were starved for 6 h in DMEM without any supplement and were pretreated with MK-801 (0.3 μM), Ro-256981 (*Ro25*, 0.5 μM), NVP-AMM077 (*NVP*, 0.5 μM), or PBS for 20 min followed by treatment with or without NMDA (100 μM) for 15 min, and whole lysates were harvested. Immunoblotting was done by using of anti-phosphorylated p38 or ERK1/2 antibodies (*p-p38, p-ERK1/2*) and anti-total p38 or ERK1/2 (*t-p38, t-ERK1/2*) antibodies, with the latter serving as an internal control for protein loading to assess the activation level of p38 and ERK1/2. *A* and *B*, representative blots from three independent experiments. *C* and *D*, scanning densitometry was quantified and normalized to control (*Con*) on the same Western blots. *, $p < 0.05$; ***, $p < 0.001$ *versus* control; #, $p < 0.05$; ###, $p < 0.001$ *versus* NMDA + PBS. Note that NMDA induced ERK1/2 activation in 3DIV neurons, and p38 activation in 12DIV neurons was significantly decreased in the presence of Ro-6981 and that the NMDA-induced weak ERK1/2 activation in 12DIV was increased in the presence of Ro-6981 but decreased in the presence of NVP-AMM077.

NR2B was already detectable at 3DIV, which increased sharply to reach peak at 9DIV and slowly came down after 12DIV. However, although the mRNA of NR2A was also detected at 3DIV, the appearance of protein was delayed until 6DIV, and it exhibited a continuous increase over time in culture until 15DIV, the last time point we have examined. Moreover, it was shown that the overall abundance of NR2B was much higher than that of NR2A during the whole development period examined, although the relative ratio of 2B/2A kept decreasing. The above expression pattern is essentially in line with previous reports that also showed the differently increased expression of NR2 subunits during development both *in vivo* (14, 45, 46) and *in vitro* (47, 48). Based on these observations in NMDARs expression, it has been suggested that the simplest explanation for the increase/appearance of NMDA neurotoxicity would be the presence of functional NMDA receptors (18, 41) and the consequent increase in NMDA-induced calcium influx in the mature neuron (36), which is sufficient to confer excitotoxic vulnerability. This argument sounds reasonable and has

become prevalent in the past decades. However, combined with several other studies, our data do not seem to support such a viewpoint.

First, the mRNA and protein of NR2B and NR2A both can be detected at 3- or 6DIV cultures in our system (Fig. 3). At these time points, neurons were resistant to NMDA toxicity, and on the contrary they favored NMDA stimulation to survive the nutrition deprivation insult (Fig. 1). Second, in these immature neurons, it is also found that NMDA can successfully trigger the ERK1/2 activation as well as calcium influx both in an NMDAR-dependent manner (Figs. 6, 8, and 9). These data strongly indicate that functional NMDA receptors already exist in immature neurons. Similar results were also seen in several other studies such as the detection of NR1 puncta in 3DIV rat cortical neurons (38) and 2DIV rat hippocampal neurons (49), as well as the NR2B-sensitive NMDA-induced whole-cell current in 1–3DIV hippocampal neurons (50). In addition, Fogal *et al.* (42) demonstrated the cell surface expression of NR1 and NR2B in 4DIV murine cortical neurons, whereas NR2A appeared only after
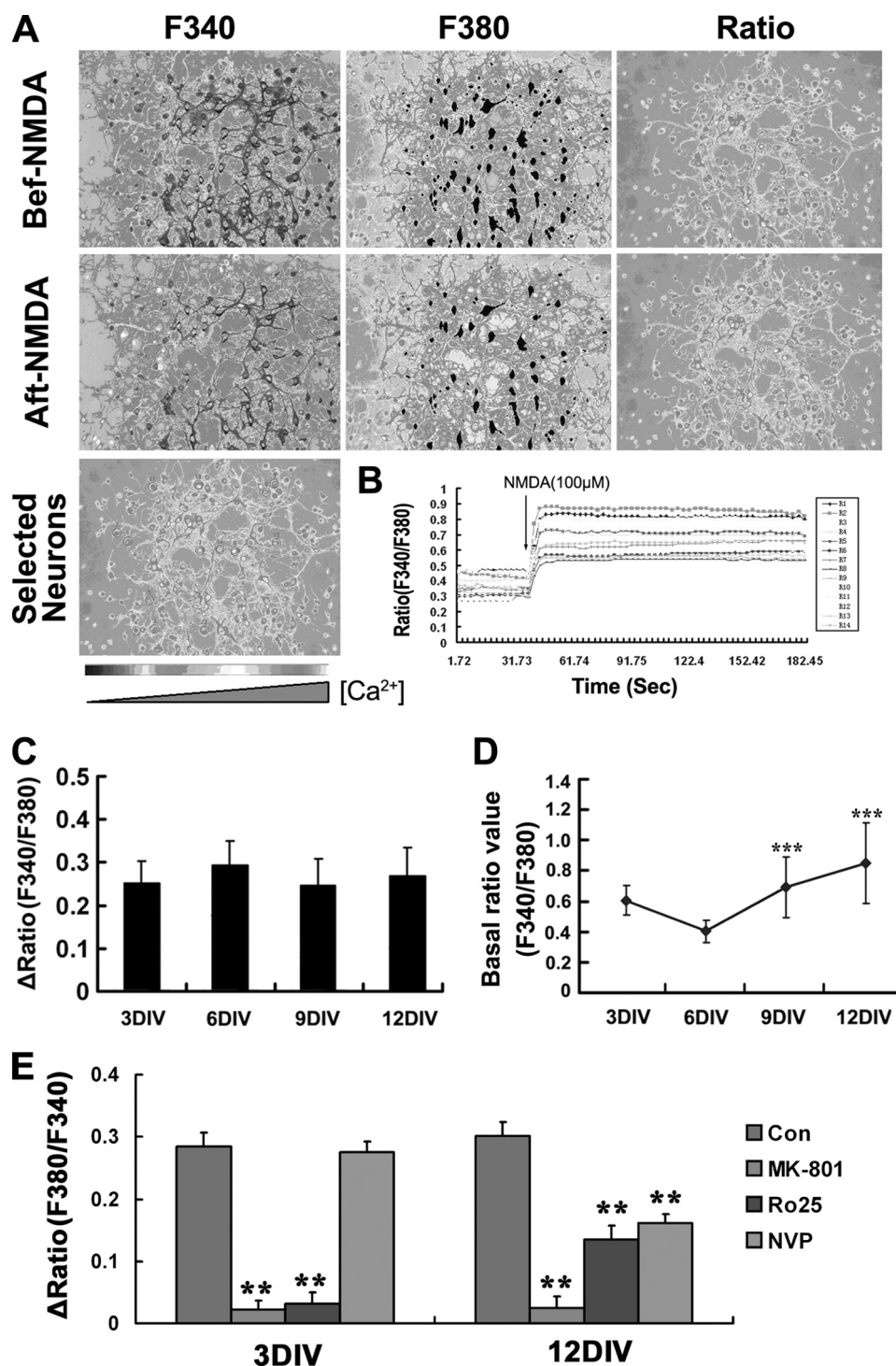
FIGURE 9. **NMDA triggers similar calcium influx both in mature and immature neurons, whereas the basal $[Ca^{2+}]_i$ level elevates with development.** *A,* representative experiment that measured the NMDA induced calcium influx in 6DIV neurons by the fura-2 method. Pseudo-colored images were captured under the indicated excitation waves. Image showed the 14 neurons that has been selected and analyzed. *B,* response curves of ratio ($F_{340/380}$) value against time of 14 selected neurons in 6DIV culture. Note that the ratio value increased immediately after addition of NMDA and was kept at the plateau levels within the experimental time range of 200 s. The ratio of fura-2 fluorescence was indicated with a gray scale bar from *black* (low $[Ca^{2+}]_i$) to *white* (high $[Ca^{2+}]_i$). *C,* amplitude of calcium influx in different developmentally staged neurons. Note that there were no obvious differences among them. *D,* basal level of intracellular free calcium increased with development. The basal ratio value of *F*340/*F*380 before NMDA stimulation was compared between neurons of different DIV. ***, $p < 0.001$ *versus* 6DIV. (328, 157, 139, and 75 total cells from 3, 6, 9, and 12 DIV points were analyzed, respectively.) *E,* effects of NMDARs antagonists on Ca^{2+} influx. At 3- or 12DIV, neurons were perfused with BSS containing MK-801 (0.3 μM), Ro-256981 (*Ro25*, 0.5 μM), NVP-AMM077 (*NVP*, 0.5 μM) or not for 2 min and then with the same BSS containing NMDA (100 μM) or not for 3–5 min. Results are from three independent experiments tracing about 120 total neurons for each data point. **, $p < 0.01$ *versus* control (*Con*). Note that NMDA-induced $[Ca^{2+}]_i$ increase in 3DIV neurons is completely blocked by Ro-6981 (*Ro25*) but is not affected by NVP-AMM077 (*NVP*), whereas the increase in 12DIV neurons significantly and completely blocked but only partially blocked both NVP-AMM077 and Ro-256981. *Bar,* 50 μm.
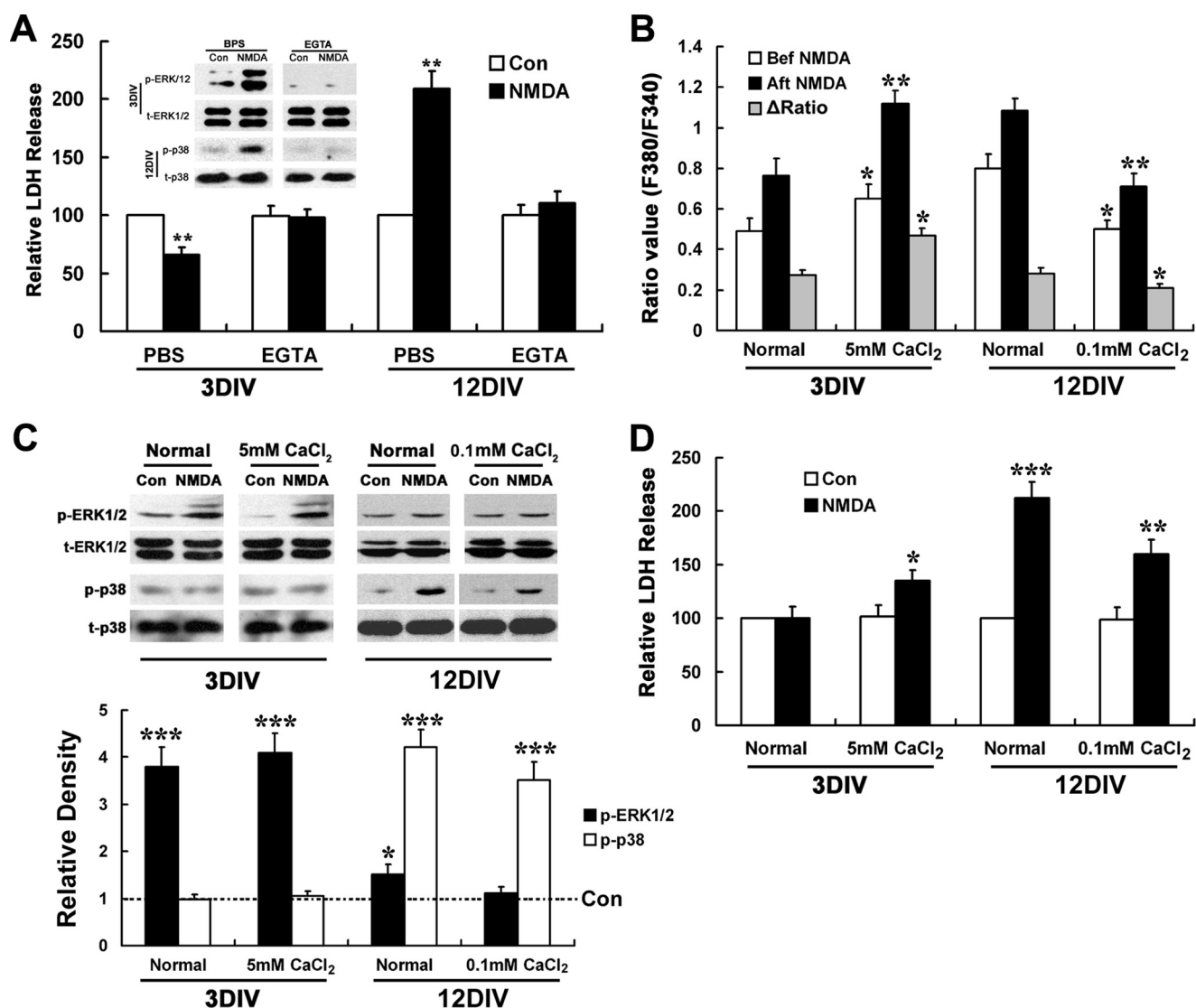
FIGURE 10. **NMDA neurotoxicity but not NMDA induced ERK1/2 and p38 MAPK activation changes according to extracellular calcium level.** For LDH release assay, 3- and 12DIV neurons were treated with or without NMDA (100 μM) for 15 min in normal or calcium-free EGTA (5 mM) containing low (0.1 mM) and high (5 mM) calcium (*A*) and Locke's solution (*D*) and washed three times with DMEM and then incubated with original culture medium (*A*, 3DIV) or DMEM for 24 h before LDH release assay. For MAPK activation, 3- and 12DIV neurons were starved in DMEM for 6 h and treated with or without NMDA (100 μM) for 15 min in normal or calcium-free EGTA (5 mM) containing low (0.1 mM) and high (5 mM) calcium (*A*) and Locke's solution (*C*). Immunoblotting was done by using anti-phosphorylated p38 or ERK1/2 antibodies (*p-p38, t-ERK1/2*) and anti-total p38 or ERK1/2 (*t-p38, p-ERK1/2*) antibodies, with the latter serving as an internal control for protein loading to assess the activation level of p38 and ERK1/2. For calcium imaging, 3- and 12DIV neurons were perfused with low (0.1 mM) or high (5 mM) calcium BSS for 2 min and then with the same BSS containing NMDA (100 μM) or not for 3–5 min. *A*, both NMDA induced neuroprotection and neurotoxicity as well as ERK1/2 and p38 activations are calcium-dependent. **, $p < 0.05$ *versus* Control (*Con*). Note that EGTA treatment abolishes both NMDA-induced neuroprotection and ERK1/2 activation in 3DIV neurons, as well neurotoxicity and p38 activation in 12DIV neurons. *B*, basal $[Ca^{2+}]_i$ in 3- and 12DIV neurons can be adjusted to a similar level by changing the extracellular concentration of $CaCl_2$. *, $p < 0.05$; **, $p < 0.01$ *versus* normal. Note the elevated basal $[Ca^{2+}]_i$ level and enhanced calcium influx in 3DIV neuron under 5 mM $CaCl_2$ condition, as well as the descended basal $[Ca^{2+}]_i$ level and decreased calcium influx in 12DIV neuron under 0.1 mM $CaCl_2$ conditions, which have no significant differences with each other. There are no significant differences in $[Ca^{2+}]_i$ levels between 3DIV neurons under normal conditions and 12DIV neurons under 0.1 mM $CaCl_2$, as well as between 12DIV neurons under normal and 3DIV neuron under 5 mM $CaCl_2$ condition both before and after NMDA stimulation. *C*, pattern of NMDA-induced activation of ERK1/2 and p38 in mature and immature neurons did not change with extracellular calcium level. Representative blots are shown from three independent experiments. *, $p < 0.05$; ***, $p < 0.001$ *versus* control. Note the dramatic activation of ERK1/2 but not p38 in 3DIV neurons under both normal and high extracellular calcium (5 mM) conditions, as well as the strong activation of p38 but not ERK1/2 in 12DIV neuron under both normal and low extracellular calcium (0.1 mM) conditions. *D*, neurotoxicity is affected by extracellular calcium levels. *, $p < 0.05$; ***, $p < 0.001$ *versus* control; **, $p < 0.01$ *versus* normal. Note that NMDA triggers significant LDH release in 3DIV neurons under 5 mM $CaCl_2$ conditions but not normal conditions, and LDH release in 12DIV neuron is significantly decreased under 0.1 mM $CaCl_2$ conditions.

7DIV. In their system, neurons were also insensitive to NMDA toxicity at these time points. Moreover, Zhou *et al.* (51) showed that NMDA stimulated a robust increase of intracellular calcium and activation of ERK1/2 and other plasticity-related signaling in 3DIV rat cortical neurons. Thus, it seemed unequivocal that fully functional NMDAR expression (at least NR1/2B

receptors) was reached prior to the development of susceptibility to NMDA neurotoxicity in our cultured hippocampal neurons, *i.e.* the mere presence of functionally mature NMDARs cannot provide complete explanation for the excitotoxic phenotype observed, and therefore other factors may as well be involved. We hypothesize it might be a matter of how NMDA

receptors function rather than whether they are functioning that determines the cell death/survival fate of different aged neurons in response to NMDA stimulation.

Switching of NMDA Receptor-favorite Intracellular Signal Pathways from ERK1/2 to p38 MAPK—It has been well documented that ERK1/2 and p38 MAPK are critical intracellular signal molecules downstreamed from NMDARs that can mediate opposite effects of glutamate in the CNS, including the regulation of synaptic plasticity and neuronal survival/death (19, 32, 33, 52). We then asked if there were any changes in the NMDA-evoked p38 and ERK1/2 activation that are coincident with the changes of NMDA neurotoxicity during maturation. In accordance with this hypothesis, it was found that NMDARs did couple differently to the above intracellular signal pathways as a function of neuronal development. Specifically, NMDA elicited significant activation of p38 MAPK in mature (9- and 12DIV) neurons but not in immature (3- and 6DIV) neurons (Fig. 6). On the contrary, it triggered dramatic ERK1/2 activation in immature (3- and 6DIV) neurons, although this ability was strikingly weakened in mature (9- and 12DIV) neurons (Fig. 6). This result demonstrated that NMDAR stimulation preferentially activated ERK1/2 in immature neurons, although it favored p38 activation in mature neurons. Consistently, *in vivo* studies also revealed that NMDA specifically activated ERK1/2 in hippocampi of P0 rats but p38 MAPK in adult rats (Fig. 7). Thus, our results indicate that there is a switch of NMDAR-favorite intracellular signaling pathways from ERK1/2 to p38 MAPK during neuronal development. This switch seemed to be a scheduled event rather than a result from nonspecific global change of intracellular signal pathways to extracellular stimulations during neuron maturation as the pattern of KCl-induced ERK1/2 and p38 MAPK activations were not changed with development (Fig. 7). Similarly, Zhou *et al.* (51) revealed that although NMDA stimulated robust ERK1/2 activation in 3DIV neurons, this effect was impaired in 14DIV neurons. Given that the majority of research has suggested a pro-survival role of ERK1/2 activation in neuronal cells (33) except several recent reports that imply a neurotoxic role (53, 54), and that p38 activation has been well documented to promote neuronal death (32, 55, 56), the changes in NMDA neurotoxicity during maturation might therefore be possibly attributed to the switch of NMDAR-favorite intracellular signaling from a pro-survival ERK1/2 pathway to a pro-death p38 MAPK pathway with development. In fact, this probability was confirmed by analysis using signal pathway-specific pharmacological inhibitors showing that NMDA neurotoxicity in mature neuron could be blocked by the p38 inhibitor SB203580 and the neuroprotection in immature neuron was blocked by ERK1/2 inhibitor PD98059 (Fig. 5). Thus, it is demonstrated that NMDA stimulation preferentially activates ERK1/2 to promote cell survival in the immature neuron, although it favors activating p38 MAPK to promote cell death in mature neurons.

The question is then what makes such a developmental switch of NMDAR-favorite signaling pathways from ERK1/2 to p38 MAPK. Because the NR2 subunit incorporation determines the property of a specific NMDAR (12, 13), and particularly because the expressions of NR2B and NR2A are differentially regulated during development with a delay in the

appearance of NR2A rather than NR2B as observed in this study (Fig. 3) and by others (14, 15, 46), it could result in the different subunit compositions of NMDARs in different aged neurons (46). Therefore, the developmental switch of the NMDAR-favorite signal pathway could be a reflection of developmental changes in NMDAR subunit compositions. This may especially be the case given that the C-terminal tails of NR2B and NR2A show considerable sequence divergence and have been reported to differentially associate with signaling molecules (57). However, by using NR2A- and NR2B-specific antagonist, our result revealed that the NMDA-induced ERK1/2 activation in 3DIV immature neurons and the p38 activation in 12DIV mature neuron were both NR2B-containing NMDAR-dependent (Fig. 8). Moreover, the corresponding NMDA neuroprotection and neurotoxicity were also both mediated by NR2B-containing NMDARs (Fig. 4). Therefore, in this system, the switch of NMDAR-favorite signal pathway from ERK1/2 to p38 and the consequent changes in NMDA neurotoxicity with development are not likely due to the developmental changes of NMDAR subunit composition as others have indicated in their systems (17).

Notably, although the NMDA-induced ERK1/2 activation was shown to be sharply weakened compare with the immature neurons, there was still a mild activation of ERK1/2 in the mature neurons that retained some pro-survival effects, as NMDA neurotoxicity in these neurons was slightly exacerbated in the presence of PD98059 (Fig. 5*C*). Interestingly, this mild ERK1/2 activation was blocked by NVP-AM077 and was enhanced by Ro-6981 (Fig. 8), suggesting that ERK1/2 activation in the mature neurons is mediated by NR2A-containing NMDARs and can be inhibited by NR2B-containing NMDARs, which is consistent with several recent reports (52, 58, 59). Thus, our results indicate that in the immature neuron, NR2B-containing NMDARs signal to activate ERK1/2 and lead to pro-survival effects, whereas in the mature neuron, NR2B-containing NMDARs switches to signal via p38 MAPK and hence leads to a pro-death effect. It is also suggested that in the mature neuron, the ERK1/2 activation is switched to couple predominantly with NR2A-containing NMDARs, whereas NR2B-containing NMDARs, instead, have adopted a role of inhibiting its activation, which may also contribute to the increased susceptibility of mature neurons to NMDA neurotoxicity in addition to the NR2B-mediated p38 MAPK activation. A schematic diagram is shown based on our study (Fig. 11).

Although numerous studies have suggested an extreme diversity of NMDAR functions, the underlying mechanism is far from completely revealed. There is no doubt that the stimulation intensity is critical to determine whether an episode of NMDAR activity is neuroprotective or excitotoxic; however, other facts that may be involved are still hotly debated. Although the results from Hardingham and co-workers (60–62) and others (63) strongly suggested a critical role of receptor location (synaptic *versus* extrasynaptic), with synaptic NMDAR activation promotes neuronal survival and extrasynaptic NMDARs activation promotes neuronal death. The laboratory of Wang and co-workers (28, 66) and others (30, 64, 65) instead presented solid data demonstrating that the receptor subunit composition (NR2B *versus* NR2A) makes sense, with NR2B

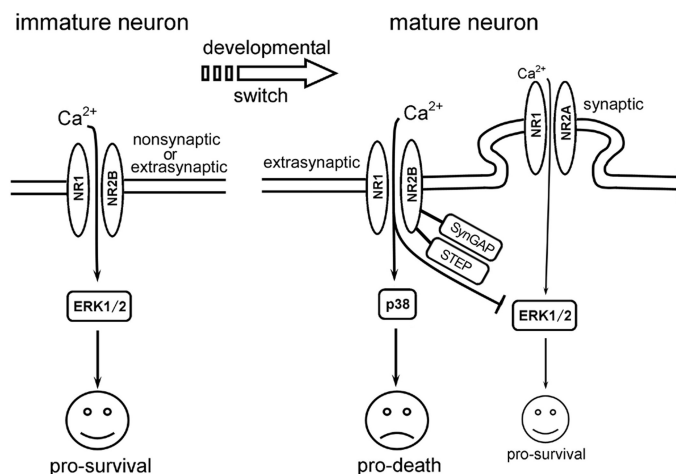# Changes of NMDAR Signaling and NMDA Neurotoxicity

FIGURE 11. **Schematic diagram for switch of NMDAR-favorite signaling and the correlative changes in NMDA neurotoxicity during development in hippocampal neurons.** In immature neurons, NR2B-containing NMDAR predominates both synaptic and extrasynaptic as well as nonsynaptic location (in early stage when synapse is hardly formed). It signals to activate ERK1/2 and leads to pro-survival effects and hence results in neuroprotection after NMDA stimulation. In mature neurons, NR2B-containing NMDARs are the predominant extrasynaptic NMDARs and signal to activate p38 MAPK, which lead to pro-death effects and results in NMDA neurotoxicity; whereas NR2A-containing NMDARs, which are the predominant synaptic NMDARs, have taken the place to activate ERK1/2 and mediated pro-survival effect. Instead, NR2B-containing NMDARs have adopted a role of inhibiting ERK1/2 activation, which might be mediated via SynGAP or/and striatally enriched tyrosine phosphatase, and further increases the susceptibility of mature neuron to NMDA neurotoxicity. The *thin line* represents a relative weak strength of the signaling. See text for detail.

coupled to pro-death signaling and NR2A coupled to pro-survival signaling. It has been suggested that in immature neurons, NR2B-containing NMDARs are predominant at both synaptic and extrasynaptic sites, whereas in mature neurons, most NR2A-containing NMDARs are incorporated in synapses and NR2B-containing NMDARs become predominant only at extrasynaptic sites (50, 67–69). Because the above-mentioned studies were mostly carried out in cultured mature neurons or in adult animals, therefore, the controversy between these data might actually be joined at this point. This is really the case when Massey *et al.* (29) clearly showed that activation of extrasynaptic NMDARs or NR2B-containing NMDARs leads to long term depression, whereas activation of synaptic NMDARs or NR2A-containing NMDARs leads to long term potentiating, although Martel *et al.* (70) reported that within a single neuron synaptic NR2B promoted neuronal survival and extrasynaptic NR2B promoted cell death, whereas Liu *et al.* (28) demonstrated that both synaptic and extrasynaptic NR2B promoted cell death, and in contrast, both synaptic and extrasynaptic NR2A promoted cell survival.

In this study, we introduced a bath application of NMDA, which resulted in the overall activation of both synaptic and extrasynaptic NMDARs. The intensity of stimulation was set at a well demonstrated neurotoxic level (100 μM, 15 min in glycine containing Locke's solution) for mature neurons in all of the mechanism analysis experiments. By using the pharmacological tools available for the time being, we attempted to dissect the individual role of different NMDAR subunits. Our result supports that in the mature neurons, global NR2B stimulation exerts a pro-death role via p38 MAPK pathway, whereas global

NR2A stimulation plays a pro-survival role via ERK1/2 pathway. But in the immature neurons, where NR2B-containing NMDARs seem to be the only subtype of functional NMDARs, the global stimulation of it leads to significant ERK1/2 activation without affecting the p38 MAPK pathway and ultimately exerts a pro-survival role. It is interesting to find that NR2B exerts opposing roles in regulation of neuronal survival as well as ERK1/2 and p38 MAPK activation depending on the developmental stage of the neuron, although the underlying mechanism is currently unknown. We suppose there is a possibility that the components and assembling of the NR2B receptor signaling complex changes with development and thus leads to the different coupling to downstream signal pathways because the expressions of many NMDA receptor-associated proteins are differently regulated and distributed during neuron maturation (49, 71). Consistently, it has been shown that extrasynaptic NMDARs coupled to the cAMP-response element-binding protein (CREB) activation pathway in 7DIV immature hippocampal neurons, although they switched to coupling with a CREB shutoff pathway in 12–14DIV mature neurons (34, 72).

The specific link of NR2B to p38 and NR2A to ERK1/2 in mature neuron observed here seems to agree with the observations of Xu *et al.* (73) that extrasynaptic NMDARs coupled preferentially to p38 and synaptic to ERK1/2 considering the predominant location of NR2B at extrasynaptic and NR2A at synaptic sites as mentioned above. Moreover, it is consistent with the findings of Li *et al.* (52) that in mature cortical neurons, NR2B specifically interacts with Ras-guanine nucleotide-releasing factor 1 (Ras-GRF1) to activate p38, whereas NR2A specifically interacts with Ras-GRF2 to activate ERK1/2, although it remains to be elucidated whether the Ras-GRFs also function similarly in the current system.

The mechanism for the inhibitory effect of NR2B on ERK1/2 activation in mature neurons is unexplored in this study. Kim *et al.* (58) have also reported that in cultured mature hippocampal neurons, extrasynaptic NMDAR strongly inactivates Ras-ERK1/2 signaling through the specific binding of NR2B with synaptic Ras GTPase-activating protein SynGAP, the role of which is to inhibit Ras activation. A similar pathway is expected to be involved in the current system. Alternatively, the NMDAR-associated striatally enriched tyrosine phosphatase, which has abundant expression in hippocampal neurons (74), is also an attractive candidate, because it is activated by the Ca^{2+}-dependent phosphatase calcineurin to directly dephosphorylate ERK (75), and this effect is shown to be NR2B-NMDAR-dependent (Fig. 11) (76). It also remains to be elucidated that how NR2B signals to activate ERK/12 in the immature neurons, especially in those 3DIV neurons, where there is seldom synapse formation. Krapivinsky *et al.* (59) suggested that NR2B can directly binds to Ras-GRF1 to activate ERK1/2 in relatively young neurons. However, Tian *et al.* (71) indicated the involvement of Sos exchange factors in immature neurons, whereas Ras-GRFs in mature neurons to mediate the NMDA-induced ERK1/2 activation. Future intensive studies on the early assembly of NMDAR signaling complex, particularly in neurons of pre-synapse formation period (such as in 3DIV), may reveal the detailed mechanism.

In brief, although the NMDA-induced ERK1/2 and p38 activations have both been extensively examined in several previous studies with different *in vitro* models (34, 77, 78), they have never been assessed concurrently in such a detailed developmental time course with large concentration ranges, and especially with regard to the NMDAR subunit contribution and the changes in NMDA neurotoxicity, using the same neuron culture system as we did in this study. Our results clearly demonstrated that switching of NMDA receptor-favorite intracellular signal pathways from ERK1/2 to p38 MAPK may be a critical determinant for the changes in NMDA neurotoxicity during development.

Relevance to Calcium Signal—As calcium influx and the consequent intracellular Ca^{2+} overloading has been suggested to be the major mediator of NMDA neurotoxicity (10, 35, 36, 79), we had expected a correlated developmental increase in the NMDA-induced Ca^{2+} influx, which might also contribute to the increased NMDA neurotoxicity. Surprisingly, NMDA triggers a remarkable and identifiable $[Ca^{2+}]_i$ increase in all developmentally staged neurons examined (Fig. 9*C*), which did not support such an expectation. Consistent with the present data, Marks *et al.* (80) have found differential sensitivity to excitotoxicity in the absence of differences in NMDA-induced calcium influx when assessed in neurons dissociated from younger (P5) and older (P22) rats. In addition, there is no difference in NMDA-induced $^{45}Ca^{2+}$ uptake between rat cerebellar granule cells of 9- and 16DIV (81), as well as between murine mixed cortical neurons of 7- and 14DIV (42); yet a higher percentage of older neurons is killed by the same stimulus. It is likely that Ca^{2+} neurotoxicity might be a function of the Ca^{2+} influx pathways that may be associated with different signal molecules in different situations rather than the Ca^{2+} loading itself, as suggested by Sattler *et al.* (82). Consistently, a growing body of evidence that points to a Jekyll and Hyde role of the NMDAR-mediated Ca^{2+} influx in the mammalian CNS (10, 37). Our data also imply that calcium influx induced by NMDA can stimulate distinct or even opposing responses, depending on the downstream pathways it links to at different developmental stages (10, 11).

Interestingly, it is found that the basal calcium level has been continuously rising with the culture age (Fig. 9*D*). Thus, although the amplitude of NMDA-induced calcium influx was essentially identical among different aged neurons because of elevated basal $[Ca^{2+}]_i$, the absolute $[Ca^{2+}]_i$ level in mature neurons would be much higher than immature ones after NMDA stimulation, which might reach a threshold to confer neurotoxicity. To test this possibility, we first confirmed the calcium dependence of all the NMDA effects observed here, including NMDA neurotoxicity and neuroprotection, as well as the ERK1/2 and p38 MAPK activation in immature and mature neurons by calcium-free assays (Fig. 10*A*). Second, by modulating the concentration of extracellular Ca^{2+} level, it is found that under high Ca^{2+} (5 mM) conditions, NMDA triggered an enhanced calcium influx in 3DIV neurons to reach a ultimate $[Ca^{2+}]_i$ level comparable with that of 12DIV neurons after NMDA stimulation under normal conditions (Fig. 10*B*), and it resulted in significant neurotoxicity, a phenomenon that was absent the 3DIV neurons under normal conditions (Fig. 10*D*).

However, it is shown that under low Ca^{2+} (0.1 mM) conditions, when the basal $[Ca^{2+}]_i$ in 12DIV neurons decreased to a similar level as that of 3DIV neurons under normal conditions, the NMDA-induced calcium influx was also hampered at levels similar to that of 3DIV neurons after NMDA stimulation under normal conditions (Fig. 10*B*), and the neurotoxicity was correlatively decreased (Fig. 10*D*). Thus, it is indicated that the elevated basal $[Ca^{2+}]_i$ level with maturation is also attributable to the developmental changes in NMDA neurotoxicity.

NMDA-induced calcium influx is critical for consequent activation of ERK1/2 and p38 MAPK, and it has been suggested to be mediated by the activation of calcineurin and calmodulin-activated protein kinase II (CaMKII) (77, 78, 83–85). It was reported that NMDA could decrease phospho-ERK1/2 in a relatively high extracellular calcium (1 mM) condition but enhanced phospho-ERK1/2 in lower extracellular calcium (0.1 mM) condition (77), suggesting that a mild elevation of $[Ca^{2+}]_i$ level was favored by EKR1/2 activation, whereas an intensive $[Ca^{2+}]_i$ elevation would instead inhibit it. This result is consistent with our observation that although immature and mature neurons showed similar amplitudes of $[Ca^{2+}]_i$ elevation in response to NMDA stimulation, the low basal calcium levels in immature neurons resulted in lower absolute $[Ca^{2+}]_i$ and was accompanied by strong activation of ERK/12, whereas the high basal calcium level in mature neurons resulted in higher absolute $[Ca^{2+}]_i$ and was accompanied by a much weaker activation of ERK1/2. Moreover, calcium is also a well known regulator of the cAMP-response element-binding protein (CREB). It has been suggested that CREB could be oppositely regulated by calcium influx mediated by differently located NMDARs and was developmentally dependent (34, 60, 72). Therefore, it is possible that NMDA-induced calcium influx links to a CREB activation signaling pathway and results in pro-survival effects in immature neurons, whereas it predominantly links to a CREB shut-off pathway and leads to pro-death effects in mature neurons (34, 60, 72).

We also explored if the elevated basal $[Ca^{2+}]_i$ level with neuron maturation was responsible for the developmental switch of NMDAR-favorite signaling pathways from ERK1/2 to p38 MAPK. It was found that there was no alteration in the patterns of NMDA-induced ERK1/2 and p38 MAPK activation in immature or mature neurons when their basal $[Ca^{2+}]_i$ was modulated to a similar level by high and low extracellular $CaCl_2$ concentrations. NMDA preferentially activated ERK1/2 in 3DIV neurons at either normal or high calcium conditions, and favored p38 activation in 12DIV neurons at either normal or low calcium conditions (Fig. 10*C*). These results indicate that the elevated basal $[Ca^{2+}]_i$ is not responsible for the switching of NMDAR-favorite signaling pathways, but it instead acts as an additional independent fact to contribute to the changes in NMDA neurotoxicity with development.

In sum, this study suggests that a switch of NMDA receptor-favorite intracellular signal pathways from ERK1/2 to p38 MAPK and the elevated basal level of $[Ca^{2+}]_i$ with age might contribute greatly to the developmental changes in NMDA neurotoxicity in hippocampal neurons. This finding may enhance our previous conception about the developmental regulation of neuronal susceptibility to excitotoxicity by pointing

out that it is not simply due to the changes in NMDAR expression, *i.e.* it might be a matter of how NMDARs function rather than whether they are functioning that determines the cell death/survival fate of neurons at different developmental stages in response to NMDA stimulation.

REFERENCES

1. Lipton, S. A., and Rosenberg, P. A. (1994) *N. Engl. J. Med.* **330,** 613–622
2. Arundine, M., and Tymianski, M. (2004) *Cell. Mol. Life Sci.* **61,** 657–668
3. Kalia, L. V., Kalia, S. K., and Salter, M. W. (2008) *Lancet Neurol.* **7,** 742–755
4. Chohan, M. O., and Iqbal, K. (2006) *J. Alzheimers Dis.* **10,** 81–87
5. Johnson, K. A., Conn, P. J., and Niswender, C. M. (2009) *CNS Neurol. Disord. Drug Targets* **8,** 475–491
6. Heng, M. Y., Detloff, P. J., Wang P. L., Tsien J. Z., and Albin, R. L. (2009) *J. Neurosci.* **29,** 3200–3205
7. Ikonomidou, C., Bosch, F., Miksa, M., Bittigau, P., Vöckler, J., Dikranian, K., Tenkova, T. I., Stefovska, V., Turski, L., and Olney, J. W. (1999) *Science* **283,** 70–74
8. Fredriksson, A., Archer, T., Alm, H., Gordh, T., and Eriksson, P. (2004) *Behav. Brain Res.* **153,** 367–376
9. Soriano, S. G., Liu, Q., Li, J., Liu, J. R., Han, X. H., Kanter, J. L., Bajic, D., and Ibla, J. C. (2010) *Anesthesiology* **112,** 1155–1163
10. Hardingham, G. E., and Bading, H. (2003) *Trends Neurosci.* **26,** 81–89
11. Hetman, M., and Kharebava, G. (2006) *Curr. Top. Med. Chem.* **6,** 787–799
12. Lynch, D. R., and Guttmann, R. P. (2001) *Curr. Drug Targets* **2,** 215–231
13. Cull-Candy, S., Brickley, S., and Farrant, M. (2001) *Curr. Opin. Neurobiol.* **11,** 327–335
14. Monyer, H., Burnashev, N., Laurie, D. J., Sakmann, B., and Seeburg, P. H. (1994) *Neuron* **12,** 529–540
15. Wenzel, A., Fritschy, J. M., Mohler, H., and Benke, D. (1997) *J. Neurochem.* **68,** 469–478
16. Liu, Z., Stafstrom, C. E., Sarkisian, M., Tandon, P., Yang, Y., Hori, A., and Holmes, G. L. (1996) *Brain Res. Dev. Brain Res.* **97,** 178–184
17. Zhou, M., and Baudry, M. (2006) *J. Neurosci.* **26,** 2956–2963
18. Mizuta, I., Katayama, M., Watanabe, M., Mishina, M., and Ishii, K. (1998) *Cell. Mol. Life Sci.* **54,** 721–725
19. Wang, J. Q., Fibuch, E. E., and Mao, L. (2007) *J. Neurochem.* **100,** 1–11
20. Xiao, L., Feng, C., and Chen, Y. (2010) *Mol. Endocrinol.* **24,** 497–510
21. Xiao, L., Qi, A., and Chen, Y. (2005) *Endocrinology* **146,** 4036–4041
22. Sherwood, N. M., and Timiras, R. S. (1970) *A Stereotaxic Atlas of the Developing Rat Brain*. University of California Press, Berkeley, CA
23. Bubeníková-Valesová, V., Balcar, V. J., Tejkalová, H., Langmeier, M., and Šťastný, F. (2006) *Neurochem. Int.* **48,** 515–522
24. Bai, J., Ramos, R. L., Ackman, J. B., Thomas, A. M., Lee, R. V., and LoTurco, J. J. (2003) *Nat. Neurosci.* **6,** 1277–1283
25. Livak, K. J., and Schmittgen, T. D. (2001) *Methods* **25,** 402–408
26. Liu, L., Wong, T. P., Pozza, M. F., Lingenhoehl, K., Wang, Y., Sheng, M., Auberson, Y. P., and Wang, Y. T. (2004) *Science* **304,** 1021–1024
27. Auberson, Y. P., Allgeier, H., Bischoff, S., Lingenhoehl, K., Moretti, R., and Schmutz, M. (2002) *Bioorg. Med. Chem. Lett.* **12,** 1099–1102
28. Liu, Y., Wong, T. P., Aarts, M., Rooyakkers, A., Liu, L., Lai, T. W., Wu, D. C., Lu, J., Tymianski, M., Craig, A. M., and Wang, Y. T. (2007) *J. Neurosci.* **27,** 2846–2857
29. Massey, P. V., Johnson, B. E., Moult, P. R., Auberson, Y. P., Brown, M. W., Molnar, E., Collingridge, G. L., and Bashir, Z. I. (2004) *J. Neurosci.* **24,** 7821–7828
30. Chen, Q., He, S., Hu, X. L., Yu, J., Zhou, Y., Zheng, J., Zhang, S., Zhang, C., Duan, W. H., and Xiong, Z. Q. (2007) *J. Neurosci.* **27,** 542–552
31. Fischer, G., Mutel, V., Trube, G., Malherbe, P., Kew, J. N., Mohacsi, E., Heitz, M. P., and Kemp, J. A. (1997) *J. Pharmacol. Exp. Ther.* **283,** 1285–1292
32. Harper, S. J., and LoGrasso, P. (2001) *Cell. Signal.* **13,** 299–310
33. Hetman, M., and Gozdz, A. (2004) *Eur. J. Biochem.* **271,** 2050–2055
34. Sala, C., Rudolph-Correia, S., and Sheng, M. (2000) *J. Neurosci.* **20,** 3529–3536
35. Hartley, D. M., Kurth, M. C., Bjerkness, L., Weiss, J. H., and Choi, D. W. (1993) *J. Neurosci.* **13,** 1993–2000
36. Cheng, C., Fass, D. M., and Reynolds, I. J. (1999) *Brain Res.* **849,** 97–108
37. MacDonald, J. F., Xiong, Z. G., and Jackson, M. F. (2006) *Trends Neurosci.* **29,** 75–81
38. King, A. E., Chung, R. S., Vickers, J. C., and Dickson, T. C. (2006) *J. Comp. Neurol.* **498,** 277–294
39. Frandsen, A., and Schousboe, A. (1990) *Int. J. Dev. Neurosci.* **8,** 209–216
40. Xia, Y., Ragan, R. E., Seah, E. E., Michaelis, M. L., and Michaelis, E. K. (1995) *Neurochem. Res.* **20,** 617–629
41. Peterson, C., Neal, J. H., and Cotman, C. W. (1989) *Brain Res. Dev. Brain Res.* **48,** 187–195
42. Fogal, B., Trettel, J., Uliasz, T. F., Levine, E. S., and Hewett, S. J. (2005) *Neuroscience* **132,** 929–942
43. McDonald, J. W., Silverstein, F. S., and Johnston, M. V. (1988) *Brain Res.* **459,** 200–203
44. Bruce, A. J., Sakhi, S., Schreiber, S. S., and Baudry, M. (1995) *Exp. Neurol.* **132,** 209–219
45. Watanabe, M., Inoue, Y., Sakimura, K., and Mishina, M. (1992) *Neuroreport* **3,** 1138–1140
46. Sheng, M., Cummings, J., Roldan, L. A., Jan, Y. N., and Jan, L. Y. (1994) *Nature* **368,** 144–147
47. Zhong, J., Russell, S. L., Pritchett, D. B., Molinoff, P. B., and Williams, K. (1994) *Mol. Pharmacol.* **45,** 846–853
48. Li, J. H., Wang, Y. H., Wolfe, B. B., Krueger, K. E., Corsi, L., Stocca, G., and Vicini, S. (1998) *Eur. J. Neurosci.* **10,** 1704–1715
49. Rao, A., Kim, E., Sheng, M., and Craig, A. M. (1998) *J. Neurosci.* **18,** 1217–1229
50. Tovar, K. R., and Westbrook, G. L. (1999) *J. Neurosci.* **19,** 4180–4188
51. Zhou, X., Moon, C., Zheng, F., Luo, Y., Soellner, D., Nuñez, J. L., and Wang, H. (2009) *J. Neurosci. Res.* **87,** 2632–2644
52. Li, S., Tian, X., Hartley, D. M., and Feig, L. A. (2006) *J. Neurosci.* **26,** 1721–1729
53. Chu, C. T., Levinthal, D. J., Kulich, S. M., Chalovich, E. M., and DeFranco, D. B. (2004) *Eur. J. Biochem.* **271,** 2060–2066
54. Chen, J., Rusnak, M., Lombroso, P. J., and Sidhu, A. (2009) *Eur. J. Neurosci.* **29,** 287–306
55. Kawasaki, H., Morooka, T., Shimohama, S., Kimura, J., Hirano, T., Gotoh, Y., and Nishida, E. (1997) *J. Biol. Chem.* **272,** 18518–18521
56. Cao, J., Semenova, M. M., Solovyan, V. T., Han, J., Coffey, E. T., and Courtney, M. J. (2004) *J. Biol. Chem.* **279,** 35903–35913
57. Kim, E., and Sheng, M. (2004) *Nat. Rev. Neurosci.* **5,** 771–781
58. Kim, M. J., Dunah, A. W., Wang, Y. T., and Sheng, M. (2005) *Neuron* **46,** 745–760
59. Krapivinsky, G., Krapivinsky, L., Manasian, Y., Ivanov, A., Tyzio, R., Pellegrino, C., Ben-Ari, Y., Clapham, D. E., and Medina, I. (2003) *Neuron* **40,** 775–784
60. Hardingham, G. E., Fukunaga, Y., and Bading, H. (2002) *Nat. Neurosci.* **5,** 405–414
61. Hardingham, G. E. (2006) *J. Physiol.* **572,** 614–615
62. Hardingham, G. E., and Bading, H. (2010) *Nat. Rev. Neurosci.* **11,** 682–696
63. Ivanov, A., Pellegrino, C., Rama, S., Dumalska, I., Salyha, Y., Ben-Ari, Y., and Medina, I. (2006) *J. Physiol.* **572,** 789–798
64. Chen, M., Lu, T. J., Chen, X. J., Zhou, Y., Chen, Q., Feng, X. Y., Xu, L., Duan, W. H., and Xiong, Z. Q. (2008) *Stroke* **39,** 3042–3048
65. Tu, W., Xu, X., Peng, L., Zhong, X., Zhang, W., Soundarapandian, M. M., Balel, C., Wang, M., Jia, N., Zhang, W., Lew, F., Chan, S. L., Chen, Y., and Lu, Y. (2010) *Cell* **140,** 222–234
66. Lai, T. W., Shyu, W. C., and Wang, Y. T. (2011) *Trends Mol. Med.*, in press
67. Stocca, G., and Vicini, S. (1998) *J. Physiol.* **507,** 13–24
68. Liu, X. B., Murray, K. D., and Jones, E. G. (2004) *J. Neurosci.* **24,** 8885–8895
69. Thomas, C. G., Miller, A. J., and Westbrook, G. L. (2006) *J. Neurophysiol.* **95,** 1727–1734
70. Martel, M. A., Wyllie, D. J., and Hardingham, G. E. (2009) *Neuroscience* **158,** 334–343
71. Tian, X., Gotoh, T., Tsuji, K., Lo, E. H., Huang, S., and Feig, L. A. (2004) *EMBO J.* **23,** 1567–1575
72. Hardingham, G. E., and Bading, H. (2002) *Biochim. Biophys. Acta* **1600,** 148–153

73. Xu, J., Kurup, P., Zhang, Y., Goebel-Goody, S. M., Wu, P. H., Hawasli, A. H., Baum, M. L., Bibb, J. A., and Lombroso, P. J. (2009) *J. Neurosci.* **29,** 9330–9343

74. Boulanger, L. M., Lombroso, P. J., Raghunathan, A., During, M. J., Wahle, P., and Naegele, J. R. (1995) *J. Neurosci.* **15,** 1532–1544

75. Paul, S., Nairn, A. C., Wang, P., and Lombroso, P. J. (2003) *Nat. Neurosci.* **6,** 34–42

76. Poddar, R., Deb, I., Mukherjee, S., and Paul, S. (2010) *J. Neurochem.* **115,** 1350–1362

77. Chandler, L. J., Sutton, G., Dorairaj, N. R., and Norwood, D. (2001) *J. Biol. Chem.* **276,** 2627–2636

78. Waxman, E. A., and Lynch, D. R. (2005) *J. Biol. Chem.* **280,** 29322–29333

79. Abele, A. E., Scholz, K. P., Scholz, W. K., and Miller, R. J. (1990) *Neuron* **4,** 413–419

80. Marks, J. D., Bindokas, V. P., and Zhang, X. M. (2000) *Brain Res. Dev. Brain Res.* **124,** 101–116

81. Eimerl, S., and Schramm, M. (1994) *J. Neurochem.* **62,** 1223–1226

82. Sattler, R., Charlton, M. P., Hafner, M., and Tymianski, M. (1998) **71,** 2349–2364

83. Zhu, J. J., Qin, Y., Zhao, M., Van Aelst, L., and Malinow, R. (2002) *Cell* **110,** 443–455

84. Komiyama, N. H., Watabe, A. M., Carlisle, H. J., Porter, K., Charlesworth, P., Monti, J., Strathdee, D. J., O'Carroll, C. M., Martin, S. J., Morris, R. G., O'Dell, T. J., and Grant, S. G. (2002) *J. Neurosci.* **22,** 9721–9732

85. Chen, H. J., Rojas-Soto, M., Oguni, A., and Kennedy, M. B. (1998) *Neuron* **20,** 895–904